

UC San Diego

UC San Diego Previously Published Works

Title

Leukotriene B4-receptor-1 mediated host response shapes gut microbiota and controls colon tumor progression

Permalink

<https://escholarship.org/uc/item/8hw2z3b0>

Journal

Oncolmmunology, 6(12)

ISSN

2162-4011

Authors

Jala, Venkatakrisna R
Maturu, Paramahamsa
Bodduluri, Sobha R
[et al.](#)

Publication Date

2017-12-02

DOI

10.1080/2162402x.2017.1361593

Peer reviewed

ORIGINAL RESEARCH



Leukotriene B₄-receptor-1 mediated host response shapes gut microbiota and controls colon tumor progression

Venkatakrishna R. Jala^{a,b,†}, Paramahansa Maturu^{a,b,†}, Sobha R. Bodduluri^{a,b}, Elangovan Krishnan^{a,b}, Steven Mathis^{a,b}, Krishnaprasad Subbarao^{a,b}, Min Wang^{a,b}, Alfred B. Jenson^c, Mary L. Proctor^d, Eric C. Rouchka^{ib e}, Rob Knight^f, and Bodduluri Haribabu^{a,b}

^aJames Graham Brown Cancer Center, University of Louisville Health Sciences Center, Louisville, KY, USA; ^bDepartment of Microbiology and Immunology, University of Louisville Health Sciences Center, Louisville, KY, USA; ^cDepartment of Pathology, University of Louisville Health Sciences Center, Louisville, KY, USA; ^dResearch Resources Center, University of Louisville Health Sciences Center, Louisville, KY, USA; ^eDepartment of Computer Engineering & Computer Science, Speed School of Engineering, University of Louisville, Louisville, KY, USA; ^fCenter for Microbiome Innovation, University of California San Diego, La Jolla, CA, USA

ABSTRACT

Inflammation and infection are key promoters of colon cancer but the molecular interplay between these events is largely unknown. Mice deficient in leukotriene B₄ receptor1 (BLT1) are protected in inflammatory disease models of arthritis, asthma and atherosclerosis. In this study, we show that BLT1^{-/-} mice when bred onto a spontaneous tumor (Apc^{Min/+}) model displayed an increase in the rate of intestinal tumor development and mortality. A paradoxical increase in inflammation in the tumors from the BLT1^{-/-}Apc^{Min/+} mice is coincidental with defective host response to infection. Germ-free BLT1^{-/-}Apc^{Min/+} mice are free from colon tumors that reappeared upon fecal transplantation. Analysis of microbiota showed defective host response in BLT1^{-/-}Apc^{Min/+} mice reshapes the gut microbiota to promote colon tumor development. The BLT1^{-/-}MyD88^{-/-} double deficient mice are susceptible to lethal neonatal infections. Broad-spectrum antibiotic treatment eliminated neonatal lethality in BLT1^{-/-}MyD88^{-/-} mice and the BLT1^{-/-}MyD88^{-/-}Apc^{Min/+} mice are protected from colon tumor development. These results identify a novel interplay between the Toll-like receptor mediated microbial sensing mechanisms and BLT1-mediated host response in the control of colon tumor development.

ARTICLE HISTORY

Received 16 May 2017
Revised 24 July 2017
Accepted 26 July 2017

KEYWORDS

Colon cancer; inflammation; BLT1; chemokines; microbiota; MyD88; host response; leukotriene B₄; inflammation and cancer


Introduction

Inflammation and infection are key promoters of cancer but the molecular interplay between these events are unclear.¹⁻⁴ Recent studies have highlighted the importance of microbiota in modulating immunity, inflammation and cancer.⁵⁻⁷ Dysbiosis-mediated inflammation has been shown to promote colon cancer progression and various mechanisms that link bacteria to tumor growth are beginning to emerge.^{6,8-10} Clinical studies outlined an association of pathogenic gut bacteria such as *Streptococcus bovis*¹¹⁻¹⁵, *Helicobacter pylori*¹⁶, *Bacteroides fragilis*¹⁷, *Escherichia coli*¹⁸, *Prevotella*⁸ and *Fusobacterium spp*¹⁹ to progression of colorectal cancer (CRC). Adenomatous polyposis coli (APC) is a well-characterized tumor suppressor and mutations in the APC gene are associated with both hereditary and sporadic colon cancers in humans.²⁰ Apc^{Min/+} mice carrying a germ-line mutation in the APC gene develop multiple polyps in the small intestine and are a widely used model for intestinal cancers.²¹ It is known that inflammation mediated by Toll-like receptors in a MyD88 dependent manner promotes intestinal tumor development in Apc^{Min/+} mice.²²

Leukotriene B₄ (LTB₄), a proinflammatory mediator produced by the rapid sequential actions of 5-lipoxygenase and leukotriene

A₄ hydrolase on arachidonic acid is a potent leukocyte chemoattractant.²³ LTB₄ mediates its effects through two G-Protein coupled receptors (GPCRs), BLT1 and BLT2.²⁴⁻²⁶ Absence of BLT1, the high affinity receptor for LTB₄, protects mice from developing inflammatory arthritis, airway hyper responsiveness and delays the progression of atherosclerosis.^{24,26-30} Recently, BLT2 was shown to mediate chemotherapy resistance in many cancer types.³¹ Since colon cancer is considered to be strongly promoted by inflammation, we crossed the BLT1^{-/-} mice³² onto the Apc^{Min/+} background²¹ to examine the role of LTB₄/BLT1 axis in the development of intestinal tumors. As with the other chronic inflammation promoted disease models, we anticipated protection from tumor development in BLT1^{-/-}Apc^{Min/+} mice. However, a paradoxical increase in inflammation and intestinal tumor development in the BLT1^{-/-}Apc^{Min/+} mice was observed. In a series of experiments, we identified that defective host response in BLT1^{-/-}Apc^{Min/+} mice translate into altered gut microbiota, increased MyD88 dependent inflammation and enhanced intestinal tumor development. The BLT1^{-/-} mice also displayed enhanced tumor burden in carcinogen (azoxymethane)-induced inflammation (dextran sodium sulfate) promoted colon tumor model. Using germ-free mice, we demonstrated that

CONTACT Bodduluri Haribabu, PhD  H0bodd01@louisville.edu  The James Graham Brown Cancer Center, CTR Bldg # 324, University of Louisville, 505-South Hancock Street, Louisville, KY-40202.

 Supplemental data for this article can be accessed on the [publisher's website](#).

[†] These authors contributed equally to this work.

colon tumor development in the BLT1^{-/-}Apc^{Min/+} is dependent on gut microbiota.

Methods

Mice

Previously described BLT1 deficient mice (> F9 on C57 BL/6 background)³² were crossed with C57BL/6-Apc^{Min/+} obtained from the Jackson Laboratory (Bar Harbor, ME) to generate BLT1^{+/+}, BLT1^{+/-} and BLT1^{-/-} in Apc^{Min/+} background. MyD88^{-/-} and MyD88^{+/-} mice in the background of BLT1^{-/-} and BLT1^{-/-}Apc^{Min/+} mice were also generated using standard breeding protocols. Mice with MyD88 deletion displayed neonatal lethality that was further exacerbated with BLT1 deletion. Breeders harbouring a MyD88^{-/-} allele (MyD88^{-/-}, BLT1^{-/-}MyD88^{-/-}, MyD88^{-/-}Apc^{Min/+} and BLT1^{-/-}MyD88^{-/-}Apc^{Min/+}) were maintained on Enrofloxacin (Baytril) at 165 mg/L in drinking water that gave a daily dosage of ~25 mg/kg until the pups are weaned between 21 and 28 d of age. All the experimental mice were maintained on regular autoclaved water and housed in ventilated cages in barrier facility under specific pathogen free conditions at the research resources center of the University of Louisville. All the experimental protocols have been approved by the Institutional Animal Care and Use Committee (IACUC) at University of Louisville.

Genotyping

DNA was extracted from tail-snips of mice using a Direct PCR lysis reagent (Viagen Biotech) according to the manufacturer's instructions. Genotyping PCR for Apc^{Min/+} was performed according to Jackson Laboratories. The genotyping PCR for BLT1 and MyD88 were performed as described previously.^{32,33}

Survival of mice

Mice (Apc^{Min/+}, BLT1^{+/-}Apc^{Min/+}, BLT1^{-/-}Apc^{Min/+}) were passively followed for long-term survival. Significance of differences in survival was determined by the Mantel-Haenszel/Log-rank test. The survival rates of the BLT1^{-/-}MyD88^{-/-} mice were calculated using data from several rounds of breeding between BLT1^{-/-}MyD88^{+/-} mice. All pups were genotyped on day 3 and percent survival rates for 3 different genotypes BLT1^{-/-}MyD88^{+/+}, BLT1^{-/-}MyD88^{+/-}, BLT1^{-/-}MyD88^{-/-} were calculated on day 15. Statistical analysis was performed by using the Mann-Whitney U test with Graph Pad Prism 4 software.

Measurement of haematocrits

The retro orbital eye bleeds (200 μ L) were collected into heparin coated microvettes (Sarstedt) and analyzed using the Hema-vet-950 Haematology System (Drew Scientific) at the indicated ages. Statistical analysis was performed using the Mann-Whitney U test with Graph Pad Prism 4.0 software.

Micro positron emission tomography (PET) imaging

Age matched (~100 d of age) Apc^{Min/+}, BLT1^{-/-}Apc^{Min/+} and BLT1^{+/-}Apc^{Min/+} were used for Micro Positron Emission Tomography (PET) imaging studies. The mice were fasted overnight (16 hours) and then injected 100 μ Ci of 9-(4-(¹⁸F)-Fluoro-3-[hydroxymethyl]butyl)guanine (¹⁸F)FHBG at 37°C. The images of these mice were collected using microPET R4 small animal and rodent PET scanner for both temporal profile of radioactivity uptake and total activity profile at the end of 1 hour. The "Acquisition Sinogram Image Processing using IDL's VirtualMachine" (ASIPRO VMTM) was used for image reconstruction and data analysis. We uniformly (Intensity ranging from 0 to 100) reconstructed transverse, coronal and sagittal images from the image file. We measured the maximum, minimum, mean, median and total activity levels in a fixed (25 pixel width x 25 pixel height) Region of Interest (ROI) in all the 3 planes.

Histopathology

Mice were killed at 2 different time points (40 d and 110 days). The entire intestinal tract was removed and flushed with 1X PBS using a blunt-end syringe to remove fecal material. The cleaned intestine divided into 4 parts consisting of the large intestine (including colon and cecum) and 3 equal length sections of the small intestine as proximal, middle and distal parts. Tissues were fixed with 10% neutral formalin and paraffin embedded. The sections were cut at 5 μ m thickness and one of the sections used for hematoxylin and eosin (H&E) and others for immunohistochemical analysis.

Enumeration of polyps

The small intestines and colons were dissected and washed with 1X PBS, longitudinally opened and spread on the filter paper and fixed in the 10% formalin for 16 hrs followed by transferring into 70% alcohol. The tumors were counted and sized under stereomicroscope containing reticule eyepiece. Polyps were categorized as <1 mm, 1–2 mm, 2–3 mm and >3 mm size. The mean number of tumors/mouse \pm SEM, and the mean tumor diameter (mm) in the group \pm SEM were calculated for the small intestine and colon separately. Statistical analysis was performed using the Mann-Whitney U test using Graph Pad Prism 4.0 software. Microadenomas in the intestines of 40 day old mice were counted and sized using Swiss-roll H&E sections under calibrated Aperio imageScope.

Immunohistochemistry (IHC)

BrdU

The proliferative activity of the cells in the polyps was determined by measuring the incorporation of 5'-bromo-2'-deoxyuridine (BrdU). Briefly, 1 ml of BrdU (1 mg/ml) was given i.p. and mice were killed after 2 hrs and intestines isolated and paraffin embedded for sectioning. IHC for the detection of BrdU was performed using BrdU *In Situ*-Detection kit from BD PharmingenTM according to manufacturer's instructions. BrdU-positive nuclei (brown nuclei) cells were manually counted per

field at 200x magnification. Statistical analysis was performed using the Mann-Whitney U test.

β-catenin and COX-2 immunohistochemistry

The β -catenin-specific mouse monoclonal antibody (Clone E-5, 1:100) and COX-2 specific Goat polyclonal antibody (clone M-19, 1:50) were used for IHC. After 1 hr incubation with the primary antibody at room temperature, the slides were washed twice with 1X PBS (5 min per wash), and then incubated with the secondary antibody solution (biotinylated goat anti-mouse IgG 1:200 for β -catenin, biotinylated donkey anti-goat IgG 1:200 for COX2) for 30 min at room temperature. Visualization of β -catenin was done by using ABC staining system (Santa Cruz Biotechnology, California). Negative controls for all staining were done by omitting primary antibodies or including isotype controls.

TUNEL

Apoptotic cells in the colon tumors were determined using terminal deoxynucleotidyl transferase-mediated nick end-labeling (TUNEL) assay. The apoptotic cells were detected using In Situ Cell Death Detection Kit, Fluorescein (Roche) according to manufacturer's instructions. The green fluorescence images were captured using Nikon Eclipse TE300 fluorescence microscope. TUNEL-positive cells were manually counted per field at 200 x magnification.

mRNA expression analysis by microarrays and real-time PCR

Total RNA was prepared from small intestine and colon tissues of WT and $BLT1^{-/-}$ mice as well as from size matched tumors of $BLT1^{-/-}Apc^{Min/+}$ and $Apc^{Min/+}$ mice (105–110 d age) using TriZol and followed by RNeasy Minikit from Qiagen. The RNA was treated with DNase using Turbo DNase kit, Ambion Inc. Microarray analysis of these samples was performed using whole mouse genome chip (Mouse 430 2.0 array, Affymetrix) according to standard protocols. Experimental and sample preparation variations were standardized by applying the global scaling procedure to all absolute analysis data using constant global target intensity. The data was analyzed using Affymetrix' MAS 5 algorithm for probe set summarization and followed by pair wise comparison. For quantitative real-time PCR, 1 μ g of total RNA was reverse transcribed in 50 μ l reaction using Taq-Man reverse transcription reagents (Applied Biosystems) using random hexamer primers. 2 μ l of cDNA and the 1 μ M real time PCR primers (Real Time Primers, LLC, Elkins Park, PA) were used in a final 20 μ l qPCR reaction with 'power SYBR-green master mix' (Applied Biosystems). Real time qPCR was performed in ABI-Prism 7900 sequence detect system (Applied Biosystems). Expression of the target genes was normalized to β -actin and displayed as fold change relative to the wild type sample. Data are representative of tumors/tissues isolated from at least 5 different mice for each genotype.

Fluorescence in situ hybridization (FISH)

To detect bacteria in the lungs of $BLT1^{-/-}MyD88^{-/-}$, the paraffin embedded cross sections of whole lungs were first de-

paraffinized and de-hydrated by sequential changes of xylene (3 times) and alcohol (100% 1 time; 95% 1 time; 70% 1 time) for 5 min. The slides were air-dried and incubated with oligonucleotide probe (5'-GCT GCC TCC CGT AGG AGT-3') complementary to a region of the 16 S rRNA, a highly conserved domain in *Bacteria*. The probe is labeled with Cy3 fluorophore at 5' end (Integrated DNA Technologies, CA). The hybridization was performed in the presence of 50 μ l of hybridization buffer (100 mM Tris-HCl, pH 8.0, 0.9 M NaCl, 35% formamide) containing Eub338 probe (5 ng/ μ l). A large coverslip was placed on the slides and carefully pressed until the hybridization solution was evenly distributed over the respective section and incubated for 1 hr in humidified chamber at 46°C. The coverslip was carefully removed and the slides were rinsed with distilled water and incubated with DAPI solution (0.5 μ g/ml) for 10 min followed by 5 min 1X PBS wash (3 times) at room temperature. The slides were mounted with aqueous anti-fade mounting media (BioMedia, CA). The fluorescence images were captured using Nikon Eclipse 80i with Texas Red/DAPI emission filter sets.

Dextran sodium sulfate (DSS) induced Colitis

Mice received 3% DSS (36–50 k_D; MP Biomedicals) in drinking water ad libitum for the duration of the experiment. The weight of the mouse was measured on Day 0 of the experiment and was used as 100% for calculating weight loss. Mice were killed and blood was removed by intracardiac puncture. The spleen, liver, mesenteric lymph nodes, and the colon including cecum were aseptically removed. The spleen, liver and mesenteric lymph nodes were stored on ice in sterile 1X PBS. The length of the colon was measured. The colon washed with 1X PBS to remove fecal matter and divided into 3 equal parts. The medial colon was opened longitudinally and washed with sterile 1X PBS and blotted to remove excess water. Each tissue was homogenized with an ultra-turrax T8 homogenizer (Ika-Werke) and serially diluted samples were plated on tryptic soy agar plates and allowed to incubate for 24 h. Colonies were counted and total CFUs were determined.

AOM/ DSS -induced colon cancer

Mice were given azoxymethane (AOM) (10 mg/kg) i.p. 7 d before administration of DSS. 2% DSS was given in drinking water in 3 cycles of 7 d on DSS followed by 14 d on normal drinking water with an additional 13 d of drinking water alone in the last cycle. Mice were killed, colons removed and the length measured. Colons were opened longitudinally and examined under a dissecting stereo microscope for tumor counting.

Generation of germ-free mice

Germ free mice ($BLT1^{-/-}$ and $BLT1^{-/-}Apc^{Min/+}$) were generated and maintained at Taconic, Germantown, NY. The mice at the age of 40 d and 110 d were killed and the polyp numbers counted and compared with specific pathogen free (SPF) animal facility at University of Louisville.

Microbiota analysis

The fecal bacterial DNA was isolated using QiAmp stool DNA isolation kit from wild type ($n = 5$), $BLT1^{-/-}$ ($n = 5$), $MyD88^{-/-}$ ($n = 5$), $BLT1^{-/-}MyD88^{-/-}$ ($n = 5$), $Apc^{Min/+}$ ($n = 8$), $BLT1^{-/-}Apc^{Min/+}$ ($n = 10$), $MyD88^{-/-}Apc^{Min/+}$ ($n = 5$), $BLT1^{-/-}MyD88^{-/-}Apc^{Min/+}$ ($n = 5$) mice. The 16 S rRNA gene V1-V3 regions was amplified using primers, 27f (AGAGTTTGATCCTGGCTCAG) and 534 r (ATTACCGCGGCTGCTGG). These primers were anchored with adapters and Multiplex Identifiers (MIDs) for 454 sequencing to distinguish various samples in a single 454 sequencing reaction. The PCR cycling conditions were 95°C for 5 min, followed by 30 cycles of 94°C for 30 seconds, 56°C for 30 seconds, and 72°C for 1 min and 30 seconds with a final extension period of 8 min at 72°C. The quadruplicate PCR amplicons were purified using AMPure magnetic bead kit and quantified using Quat-iT Picogreen kit. The amplicons were divided into 6 groups, where each group contains 10 individual samples containing unique MIDs incorporated into primer sequences. The pooled amplicons sequenced using 454/Roche GS FLX system or 454Roche Jr according to manufacturer's protocols. The microbiota data analysis was performed using QIIME platform scripts (www.qiime.org). The sequences were rarefied at randomly selected 2000 sequences and further downstream analysis was performed. The microbial classification was performed using GreenGenes reference database (gg_13_8_otus) using QIIME tools (www.qiime.org).³⁴ The sequences reference picked into Operational Taxonomic Units (OTUs) by clustering 97% sequence similarity (uclust) using the GreenGenes reference data set gg_13_8_otus and classified at various taxonomic ranks (phylum, order, class, family, genus, and species). We generated the α -diversity plots (which describe the richness and/or evenness of taxa in a single sample) and the β diversity principle coordinate plots generated using phylogenetic metrics generated using UniFrac distances using QIIME pipeline.³⁵

Semi-quantification of *Akkermansia muciniphila* by real time PCR

The real time PCR primers targeting variable regions of 16 S rRNA gene of *Akkermansia muciniphila* (FP: 5' GCCTCAGCGTCAGTTAATGT 3', RP: 5' AGGCTGTTTCG-TAAGTCGTG 3') were synthesized. Universal primers (FP: 5' TGCA YGGYYGTCSTCAGCTCGTG 3' RP: 5' TGACGT-CYTCCRCYCCTTCCTC 3') were used to normalize the levels of total bacteria in the sample. Total fecal DNA (1 ng) was used as template in 20 μ l SyBR (Applied Biosystems) reaction mixture and the RT PCR was performed at 50°C for 2 min and then 95°C for 10 min and followed by 40 cycles at 95°C for 10 seconds and 58°C for 45 seconds. The PCR reactions were subjected to heat dissociation protocol present in ABI prism 7900 sequence detection system to confirm the presence of single and unique PCR product. Reaction mixtures without genomic DNA were also used as negative controls to confirm the absence of primer-dimer formation. The relative amount of DNA is compared with control (average of 4 samples of

$Apc^{Min/+}$ fecal DNA) using $2^{-\Delta\Delta Ct}$ method³⁶ by normalizing with universal primer PCR product in all the experiments. The real time PCR products were purified and sequenced to confirm the authenticity of products belongs to intended bacteria.

Intestinal permeability assay

The gut barrier integrity was assessed by intestinal permeability assay using FITC-dextran ($MW_{av} = 4000$; FD4). The mice were fasted overnight. The FD4 (80 mg/mL PBS) was administered by oral gavage (600 mg/kg bodyweight) to fasted mice. The plasma was collected after 2 h and the FD4 leakage was measured on a fluorescence plate reader.

Results

Accelerated mortality and tumorigenesis in $BLT1^{-/-}Apc^{Min/+}$ mice

To examine the function of BLT1 in intestinal tumorigenesis, $BLT1^{-/-}$ mice were crossed to $Apc^{Min/+}$ mice to generate compound mice. The $BLT1^{-/-}Apc^{Min/+}$ mice on an identical genetic background and housing conditions displayed a significant increase in mortality relative to $Apc^{Min/+}$ mice (Fig. 1A). Littermate heterozygous mice ($BLT1^{+/-}Apc^{Min/+}$) showed intermediate survival patterns suggesting a gene dosage dependent effect. The life expectancy of $BLT1^{-/-}Apc^{Min/+}$ at 102 d was $\sim 30\%$ less than the 156 d for $Apc^{Min/+}$ mice. Progression of intestinal tumors is associated with severe anemia in $Apc^{Min/+}$ mice. Analyses of haematocrit showed that age matched $BLT1^{-/-}Apc^{Min/+}$ mice were severely anemic relative to $Apc^{Min/+}$ mice (Fig. 1B). Micro Positron Emission Tomography (MicroPET) imaging indicated higher levels of metabolic activity in the intestines of $BLT1^{-/-}Apc^{Min/+}$ compared with $Apc^{Min/+}$ mice (Supplementary Fig. 1). Age matched (~ 110 days) $BLT1^{-/-}Apc^{Min/+}$ mice showed significantly increased number of tumors compared with $Apc^{Min/+}$ mice in the small intestine and the colon (Fig. 1C-D and Supplementary Figure 2A, B). Most notably, there is a predominance of larger tumors both in small intestines (> 1 mm) and in colons (> 3 mm) of the $BLT1^{-/-}Apc^{Min/+}$ mice (Fig. 1E and Supplementary Figure 2C). Several large tumors are clearly visible in the colons of $BLT1^{-/-}Apc^{Min/+}$ mice with many of them nearly occluding the lumen (Fig. 1F). Thus, it is evident that tumors are initiated at much higher rate and grew larger in $BLT1^{-/-}Apc^{Min/+}$ mice. In $Apc^{Min/+}$ mice intestinal tumors are initiated by the loss of heterozygosity during the first few weeks of life.³⁷ To examine the role of BLT1 at early stage of tumorigenesis, we assessed tumor formation at the age of 40 d in $Apc^{Min/+}$ and $BLT1^{-/-}Apc^{Min/+}$. There is detectable anemia, an indirect marker for tumor burden in these mice that is significantly more in $BLT1^{-/-}Apc^{Min/+}$ mice relative to $Apc^{Min/+}$ mice (Supplementary Figure 3A). Consistent with this finding, histopathological examination showed the presence of more micro adenomas in the small intestines of $BLT1^{-/-}Apc^{Min/+}$ mice (Supplementary Figure 3B, D) compared with $Apc^{Min/+}$ mice. While there were no detectable colon tumors in $Apc^{Min/+}$ mice at this stage, several colon tumors including some large tumors were observed in $BLT1^{-/-}Apc^{Min/+}$ mice (Supplementary Figure 3C, E).

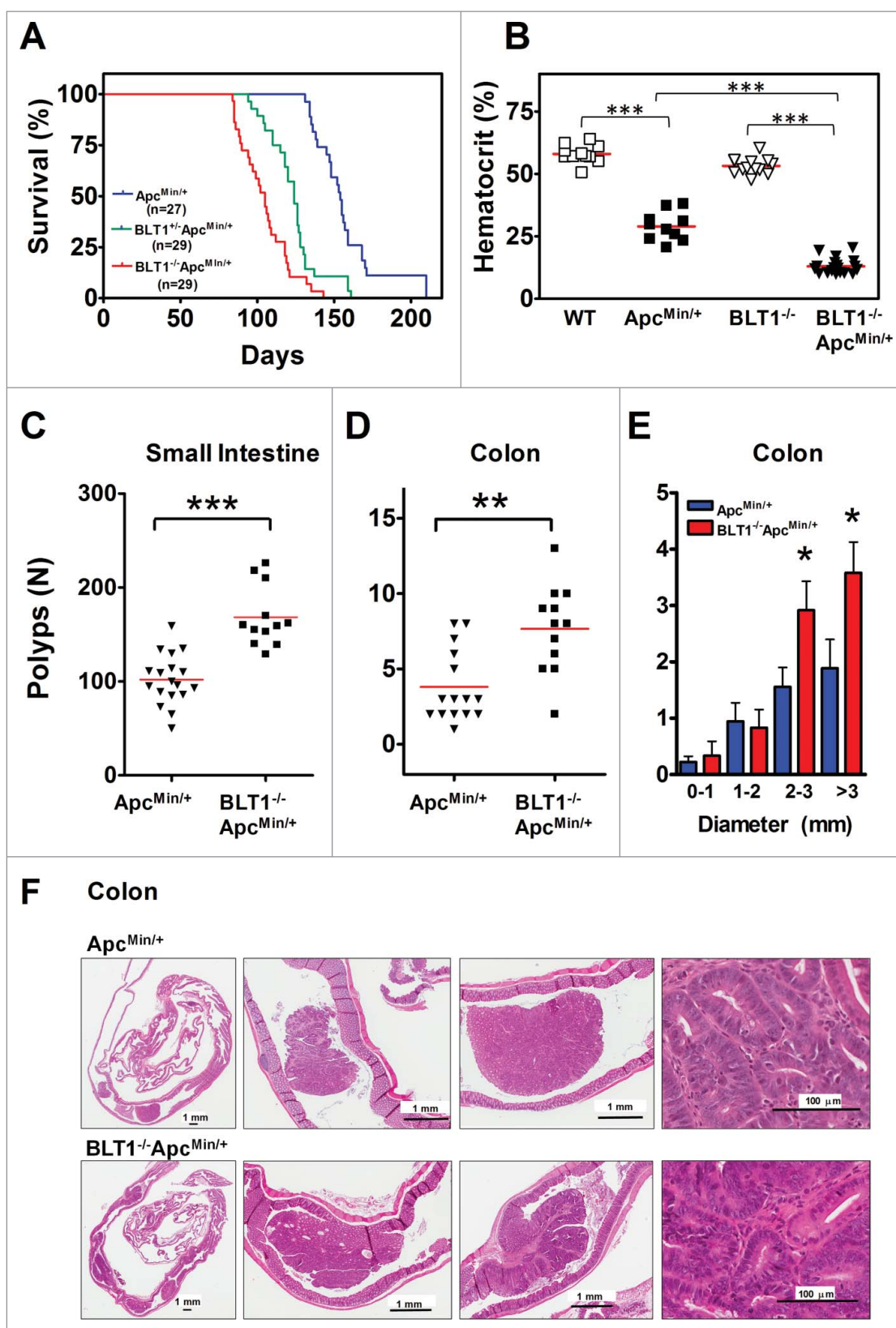


Figure 1. Increased mortality and tumorigenesis in $BLT1^{-/-}Apc^{Min/+}$ mice. (A) Kaplan-Meier plot of survival from $Apc^{Min/+}$ (n = 27) (blue), $BLT1^{+/-}Apc^{Min/+}$ (n = 29) (green), and $BLT1^{-/-}Apc^{Min/+}$ mice (n = 29) (red) are shown. Difference in survival of $Apc^{Min/+}$ mice compared with other 2 strains was determined to be significant by the Mantel-Haenszel/Log-rank test ($P < 0.0001$). (Mean survival for $Apc^{Min/+}$ (156 days), $BLT1^{+/-}Apc^{Min/+}$ (126 days), and $BLT1^{-/-}Apc^{Min/+}$ (102 days)). (B) Severe anemia in $BLT1^{-/-}Apc^{Min/+}$ mice. Hematocrit values were determined for the indicated mice at the age of ~110 d. Statistical analysis was performed using Mann-Whitney U test ($*** = P < 0.001$). (C-F) Increased intestinal tumor burden in $BLT1^{-/-}Apc^{Min/+}$ mice. Total number of polyps in the small intestine (C) and colon (D) were quantified by stereoscopic microscopy in age matched (100–110 d old) $Apc^{Min/+}$ (n = 18) and $BLT1^{-/-}Apc^{Min/+}$ (n = 12) mice using longitudinally opened tissue sections. (E) The size distribution of colon tumors in $Apc^{Min/+}$ (blue bar) and $BLT1^{-/-}Apc^{Min/+}$ (red bar) was measured. There was a significant increase in the large sized tumors (> 2 and >3 mm) in $BLT1^{-/-}Apc^{Min/+}$ when compared with $Apc^{Min/+}$. Statistical analysis was performed using Mann-Whitney U test. Error bars, \pm SEM. *, $P < 0.05$; **, $P < 0.01$; and ***, $P < 0.001$. (F) Representative cross section images of colons stained with Hematoxylin and Eosin (H&E) shows increased number and size of tumors in $BLT1^{-/-}Apc^{Min/+}$ compared with $Apc^{Min/+}$. Images were captured using Aperio Image scope, Aperio Technologies Inc.

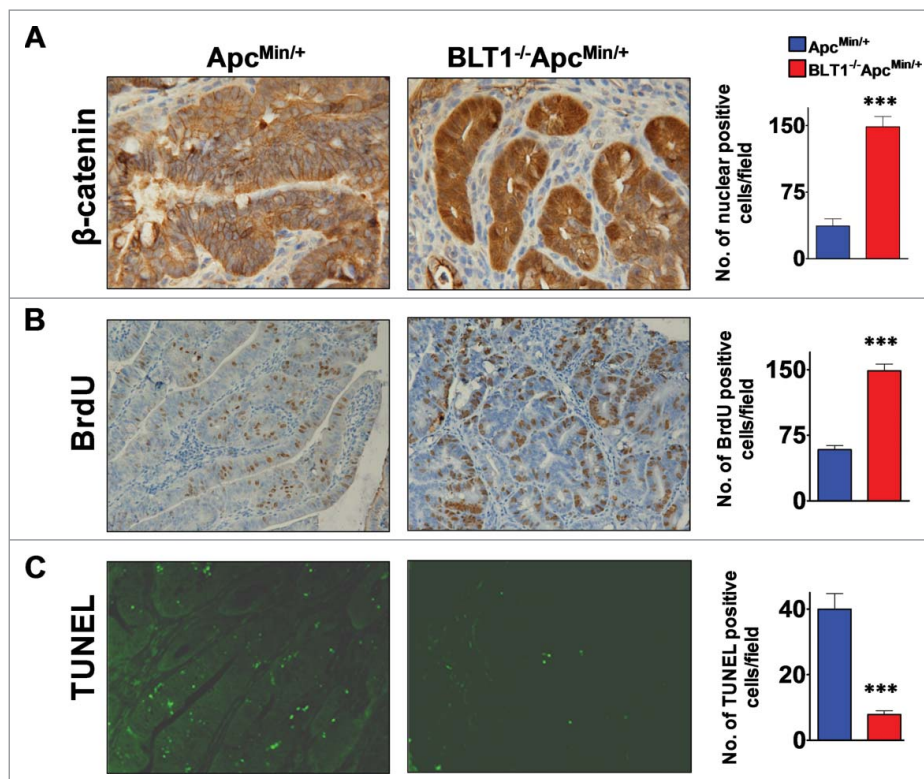


Figure 2. Analysis of β -catenin localization, proliferation and apoptosis in BLT1^{-/-}Apc^{Min/+} tumors. (A) IHC analysis of β -catenin staining of colon adenomas of Apc^{Min/+} and BLT1^{-/-}Apc^{Min/+} mice. The polyps from the BLT1^{-/-}Apc^{Min/+} mice showing more intense nuclear localization of β -catenin relative to the colon polyps Apc^{Min/+}. (B) 5-bromo-2-deoxyuridine (5-BrdU) injected into mice 2 hrs before sacrificing the mice. The cross section of colons stained with BrdU antibody. Immunohistochemical (IHC) analysis of 5-BrdU-incorporation showed a significant increase in the number of proliferating cells in colonic polyps of BLT1^{-/-}Apc^{Min/+} mice. (C) Terminal deoxynucleotidyl Transferase Biotin-dUTP Nick End Labeling (TUNEL) stain performed on colons of Apc^{Min/+} and BLT1^{-/-}Apc^{Min/+} mice. The number of TUNEL positive apoptotic cells are significantly decreased in BLT1^{-/-}Apc^{Min/+} tumors compared with Apc^{Min/+} mice. Statistical analysis was performed using Mann-Whitney U test. Error bars, \pm SEM and ***, $P < 0.001$.

Increased proliferation and decreased apoptosis in BLT1^{-/-}Apc^{Min/+} tumors

Since colonic tumors appear earlier and progress more rapidly in BLT1^{-/-}Apc^{Min/+} mice relative to Apc^{Min/+} mice, it is possible that molecular events required for the initiation and progression are accelerated in these mice. To explore these mechanisms, we determined the nuclear translocation of β -catenin, rates of proliferation and apoptosis in size matched tumors from BLT1^{-/-}Apc^{Min/+} mice and Apc^{Min/+} mice. Colon tumors from BLT1^{-/-}Apc^{Min/+} mice displayed an increase in β -catenin nuclear localization (Fig. 2A), an increase in rate of proliferation (increase in BrdU positive cells) (Fig. 2B) as well as a decrease in apoptosis (decrease in TUNEL positive cells) compared with tumors from Apc^{Min/+} mice (Fig. 2C). These results demonstrate that activities associated with rapid tumor development are increased in the tumors from BLT1^{-/-}Apc^{Min/+} mice.

Enhanced colitis associated colon tumor development in BLT1^{-/-} mice

Inflammatory bowel diseases (IBDs) such as Crohn's disease and ulcerative colitis are often associated with progression to colon cancer development in humans.³⁸ In mice, treatment with DSS induces colitis, presumably due to direct epithelial damage and ensuing inflammation. To examine the role of BLT1 in colitis, we subjected the BLT1^{-/-} mice to the DSS model. Mice were given 3% DSS in drinking water and monitored for weight loss and survival over a

15 day period. The BLT1^{-/-} mice are more susceptible to DSS-induced colitis and significant loss of body weight compared with WT mice (Fig. 3A). The shortening of colon lengths is one of the hallmarks of colitis due to increased inflammation. The colon lengths of DSS-treated BLT1^{-/-} mice were significantly reduced compared with DSS-treated WT mice (Fig. 3B). The histopathological examination of colons (distal, medial, and proximal) showed significantly greater loss of crypts in BLT1^{-/-} mice compared with WT (Supplementary Figure 4). A portion of the colon, the mesenteric lymph nodes (MLN), spleen, and liver from the DSS-treated mice were analyzed for the total tissue bacterial content on tryptic soy agar (TSA) for aerobic and TSA Blood Agar for anaerobic bacteria. The total bacterial loads [colony-forming units (CFUs)] in various organs in DSS-treated mice indicated that BLT1^{-/-} mice has increased systemic bacterial burden compared with WT mice (Fig. 3C). DSS-induced colitis strongly promotes AOM-induced colon cancer in mice.⁴ In AOM-DSS colon tumor model, the BLT1^{-/-} mice showed a significant increase in colon tumor development (Fig. 3D and E). Overall, these studies suggest that absence of BLT1 significantly increased DSS-induced inflammation and promotes carcinogen induced colon tumors.

Defective host-response in tumors from BLT1^{-/-}Apc^{Min/+} mice

Increased inflammation promotes development of intestinal tumors.^{1,4,39} Genes involved in promoting inflammation and

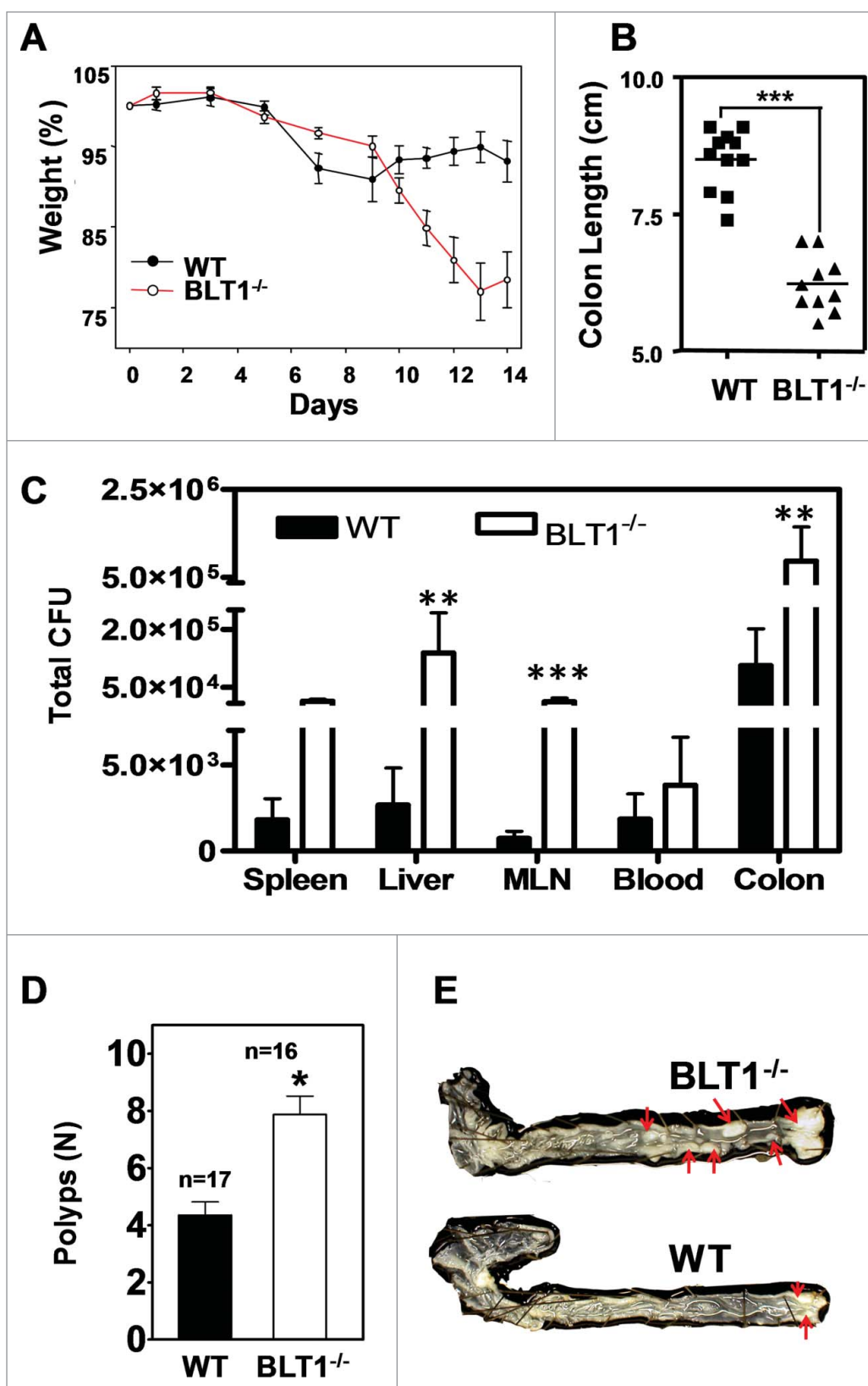


Figure 3. BLT1^{-/-} mice are more susceptible to DSS induced colitis and AOM/DSS induced colon tumorigenesis. Wild type (WT) and BLT1^{-/-} mice received 3% DSS in drinking water ad libitum for the duration of the experiment. (A) The bodyweights of wild type (n = 10) and BLT1^{-/-} (n = 8) mice were measured every 2 d for 2 weeks using weight at Day 0 of the experiment as 100% for calculating weight loss. (B) The mice were killed at day 14 and colon length of BLT1^{-/-} (n = 10) was significantly reduced compared with wild type mice (n = 11). (C) Tissue bacterial loads of DSS treated Wild type (n = 8) and BLT1^{-/-} (n = 8) mice. The spleen, liver, mesenteric lymph nodes, and the colon were aseptically removed and each tissue was then homogenized in sterile 1X PBS and was serially diluted and plated on tryptic soy agar plates and incubated for 24 hrs at 37°C. Colonies were counted and total CFUs were determined based on the total volume of the specimens. (D-E) Increased incidence of azoxymethane (AOM)/DSS induced colon cancer in BLT1^{-/-} mice. The number of polyps in colon increased in BLT1^{-/-} mice treated with AOM/DSS (D), and representative colon images of AOM-DSS treated BLT1^{-/-} and BLT1^{+/+} mice are shown (E). The red arrows point to visible tumors. Statistical analysis was performed using the Mann-Whitney U test. Error bars, ± SEM. *, P < 0.05; **, P < 0.01; and ***, P < 0.001.

tissue repair are upregulated in $Apc^{Min/+}$ tumors in a MyD88 dependent manner.²² Therefore, we measured the mRNA levels of inflammatory markers and positive regulators of tumorigenesis such as tumor necrosis factor- α (TNF- α), interleukin (IL)-6, CXCL1/KC and cyclooxygenase-2 (COX-2)^{4,40} in size-matched tumors from the colon of $BLT1^{-/-}Apc^{Min/+}$ and $Apc^{Min/+}$ (Fig. 4A). The data shows that IL-6, CXCL1/KC, TNF- α and COX2 are elevated in tumors from $BLT1^{-/-}Apc^{Min/+}$ compared with $Apc^{Min/+}$ mice. The increase in COX2 expression in $BLT1^{-/-}Apc^{Min/+}$ tumors relative to $Apc^{Min/+}$ tumors was also observed by IHC (Fig. 4B and Supplementary Figure 5). Increased intestinal tumorigenesis in $BLT1^{-/-}Apc^{Min/+}$ mice may be directly related to the increased inflammation.

The increase in inflammation in tumors from $BLT1^{-/-}Apc^{Min/+}$ raises a critical question; why the loss of a pro-inflammatory mediator (LTB₄-BLT1 axis) increased inflammation in this instance, whereas loss of BLT1 reduced inflammation in models of asthma, arthritis and atherosclerosis.²⁶⁻³⁰ To explore the potential mechanisms, global changes in gene expression profiles in these tumors were determined using microarrays. In addition to increased expression of inflammatory/tumor promoting markers such as IL-6, KC, COX2, etc., the array analysis also revealed a novel pattern of genes that are downregulated in tumors from $BLT1^{-/-}Apc^{Min/+}$ mice relative to $Apc^{Min/+}$ mice. In particular, the top 10 genes that were downregulated included angiogenins (Ang1 and Ang4), indoleamine-pyrole 2, 3 dioxygenase (IDO), and regenerating islet-derived 3 γ (Reg III γ , REG3G) (Supplementary Fig. 6). Each of these proteins was shown to possess strong direct bactericidal activity.⁴¹⁻⁴⁶ Angs and Reg3 g display specific killing activity on gram-positive bacteria such as *Listeria monocytogenes* and *Enterococcus faecalis*. The relative expression of these genes determined in the individual tumor samples shows a direct contrast with the up regulation of inflammatory markers (Fig. 4). The angiogenin mRNA levels (Fig. 4C) were also consistent with the changes in protein levels determined using a common Ang-specific antibody by Western blotting (Fig. 4D).

Germ-free $BLT1^{-/-}Apc^{Min/+}$ mice are free of colon cancer

LTB₄-BLT1 axis has been implicated in protection against bacterial and viral infections by producing anti-microbial proteins and peptides.⁴⁷⁻⁵⁰ To examine the role of BLT1 and microbiota mediated host response in colon tumor progression, germ free $BLT1^{-/-}Apc^{Min/+}$ mice were generated. The germ-free $BLT1^{-/-}Apc^{Min/+}$ mice showed complete absence of colon polyps (Fig. 5A). Recolonizing these mice at the age of 50 d with fecal bacteria from specific pathogen free (SPF) $BLT1^{-/-}Apc^{Min/+}$ mice led to the development of several colon polyps by 110 d indicating a critical role for fecal bacteria in promoting colon cancer (Fig. 5B). The germ-free mice developed similar level of small intestinal polyps as mice housed under SPF condition (Fig. 5C-D). Histopathological examination also confirms the complete absence of colon tumors and similar levels of small intestinal tumors in germ-free mice relative to mice maintained under SPF conditions (Fig. 5E).

MyD88 is essential for promoting tumor development in $BLT1^{-/-}Apc^{Min/+}$ mice

MyD88 plays an important role in host defense and was shown to be a critical mediator of tumor promoting inflammation.^{22,51} This is in contrast with the LTB₄/BLT1 axis, which also appears to be important in host defense but seems to offer protection against tumor development. To examine the interplay of host defense and tumor promotion, we crossed $MyD88^{-/-}$ mice with $BLT1^{-/-}$ to generate double deficient mice. The 3 possible offspring from the $BLT1^{-/-}MyD88^{+/-}$ crosses are born at the expected Mendelian ratios but all the double deficient ($MyD88^{-/-}BLT1^{-/-}$) mice died very early with few pups living up to 14 d (Fig. 6A). The double deficient mouse which survived the longest was very sick and half the size of its heterozygous littermate (Fig. 6B). Histopathological and microbiological examination showed infections of multiple organs including lungs and liver. The massive lung infections were delineated by Fluorescence In Situ Hybridization (FISH) analysis with bacterial probes (Fig. 6C). Microbiological examination showed that the death of some of the double deficient mice could be attributed to *Pasteurella pneumotropica* infection that does not seem to affect the littermate heterozygous and WT animals. Treatment with a broad spectrum antibiotic, Baytril, completely protected the $MyD88^{-/-}BLT1^{-/-}$ mice from neonatal lethality (Fig. 6A).

Since the $BLT1^{-/-}MyD88^{-/-}$ mice could be kept alive by treatment with broad spectrum antibiotics, we generated $BLT1^{-/-}MyD88^{-/-}Apc^{Min/+}$ mice to examine the role of MyD88 mediated inflammation in tumor promotion in the $BLT1^{-/-}Apc^{Min/+}$ mice. As control, we also developed $MyD88^{-/-}Apc^{Min/+}$ mice. As reported earlier,²² the $MyD88^{-/-}Apc^{Min/+}$ mice are highly protected with normal haematocrit (Fig. 6D) and greatly reduced tumor burden in both small intestines and colon (Fig. 6E, F). Analysis of tumor development in $BLT1^{-/-}MyD88^{-/-}Apc^{Min/+}$ mice showed that MyD88 dependent signaling is essential for the acceleration of tumor development seen in the $BLT1^{-/-}Apc^{Min/+}$ mice (Fig. 6 G-I). These results suggest that MyD88 acts downstream of BLT1 in tumor promotion and the absence of BLT1 likely results in enhanced activation of MyD88 dependent signaling.

Microbiota promotes colon tumorigenesis in $BLT1^{-/-}Apc^{Min/+}$ mice

Since germ-free mice were completely protected from colon tumor development, we examined the gut microbiota in Wild type, $BLT1^{-/-}$, $Apc^{Min/+}$, $BLT1^{-/-}Apc^{Min/+}$ along with $MyD88^{-/-}$ mice in the above backgrounds by 16 S rRNA gene sequencing. The fecal bacteria are majorly composed of *Bacteroidetes* and *Firmicutes* accounting up to ~80% (Fig. 7A) total bacteria. The levels of *Firmicutes* and *Verrucomicrobia* significantly increased (26.8% vs 18%; 7.3% vs 2.1%) and levels of *Bacteroidetes* were significantly decreased (57.7% vs 52%) in $BLT1^{-/-}Apc^{Min/+}$ compared with $Apc^{Min/+}$ (Fig. 7A).

The analysis at genus levels indicated an overall significant increase in anaerobic bacteria, *Akkermansia muciniphila* in $BLT1^{-/-}Apc^{Min/+}$ compared with $Apc^{Min/+}$ mice fecal samples (Fig. 7B). Increased levels of *Akkermansia muciniphila* in

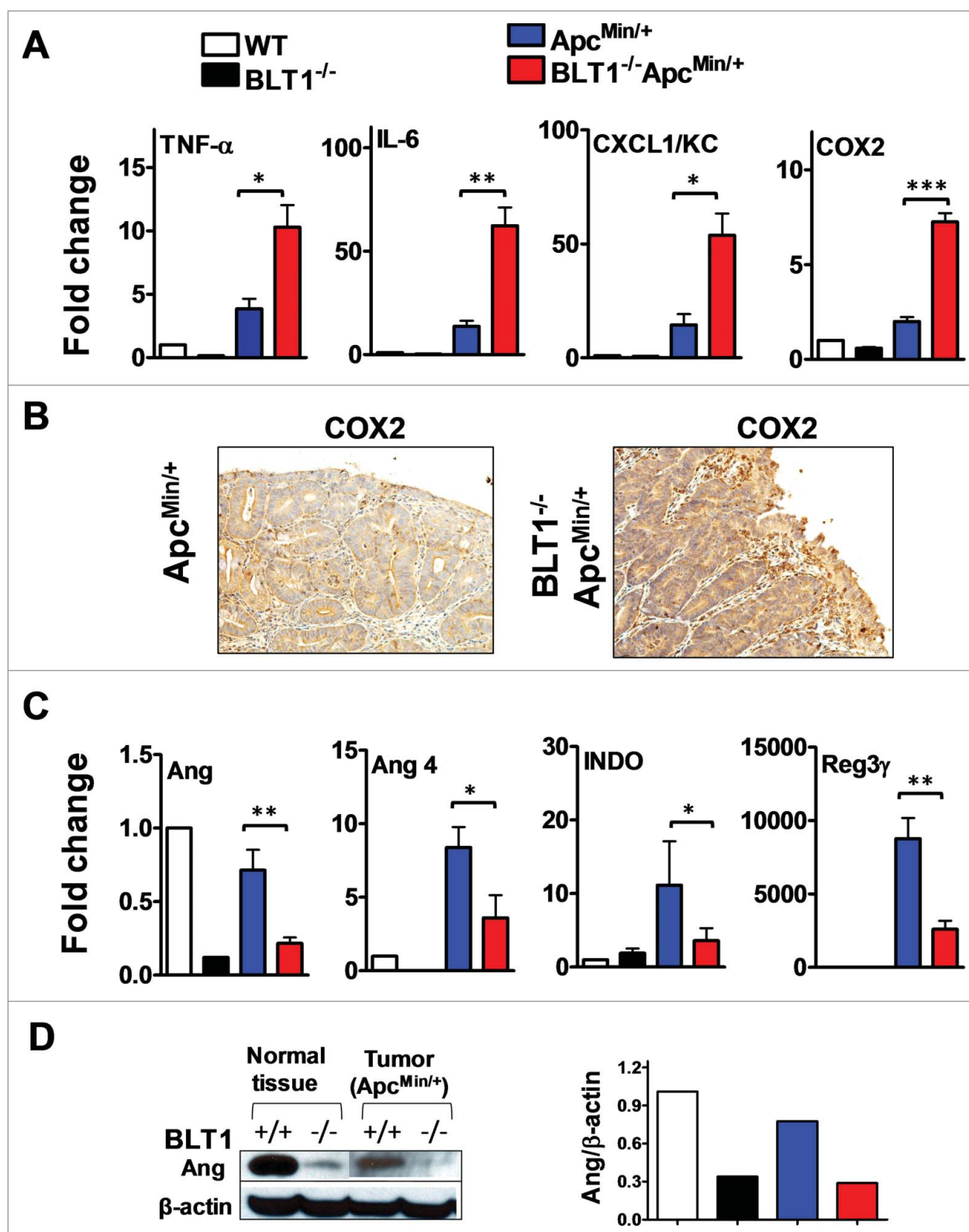


Figure 4. Increased inflammatory and decreased host defense markers in $BLT1^{-/-}Apc^{Min/+}$ tumors. (A-B). The mRNA levels were measured by qRT-PCR using SyBR green dye (Applied Biosystems) from size matched colon tumors of $Apc^{Min/+}$ and $BLT1^{-/-}Apc^{Min/+}$ mice (105–110 d age old). Data are representative of tumors/tissues isolated from at least 5 different mice for each genotype. (A). mRNA levels of inflammatory mediators (TNF- α , IL-6, CXCL1 and COX2) are significantly increased in colonic tumors of $BLT1^{-/-}Apc^{Min/+}$ compared with $Apc^{Min/+}$ mice. Statistical analysis was performed using the Mann-Whitney U test. Error bars, \pm SEM. *, $P < 0.05$; **, $P < 0.01$; and ***, $P < 0.001$ (compared with $Apc^{Min/+}$). (B). Immunohistochemical analysis indicates increased expression of COX2 in the colon tumors of $BLT1^{-/-}Apc^{Min/+}$ compared with $Apc^{Min/+}$ mice. (C) The relative mRNA levels of host defense proteins (Ang, Ang 4, IDO and Reg3 γ) were reduced in $BLT1^{-/-}Apc^{Min/+}$ compared with $Apc^{Min/+}$ mice colon tumors. (D) Western blot analysis of angiogenin expression in colons and colon tumors of $BLT1^{-/-}Apc^{Min/+}$ compared with $Apc^{Min/+}$.

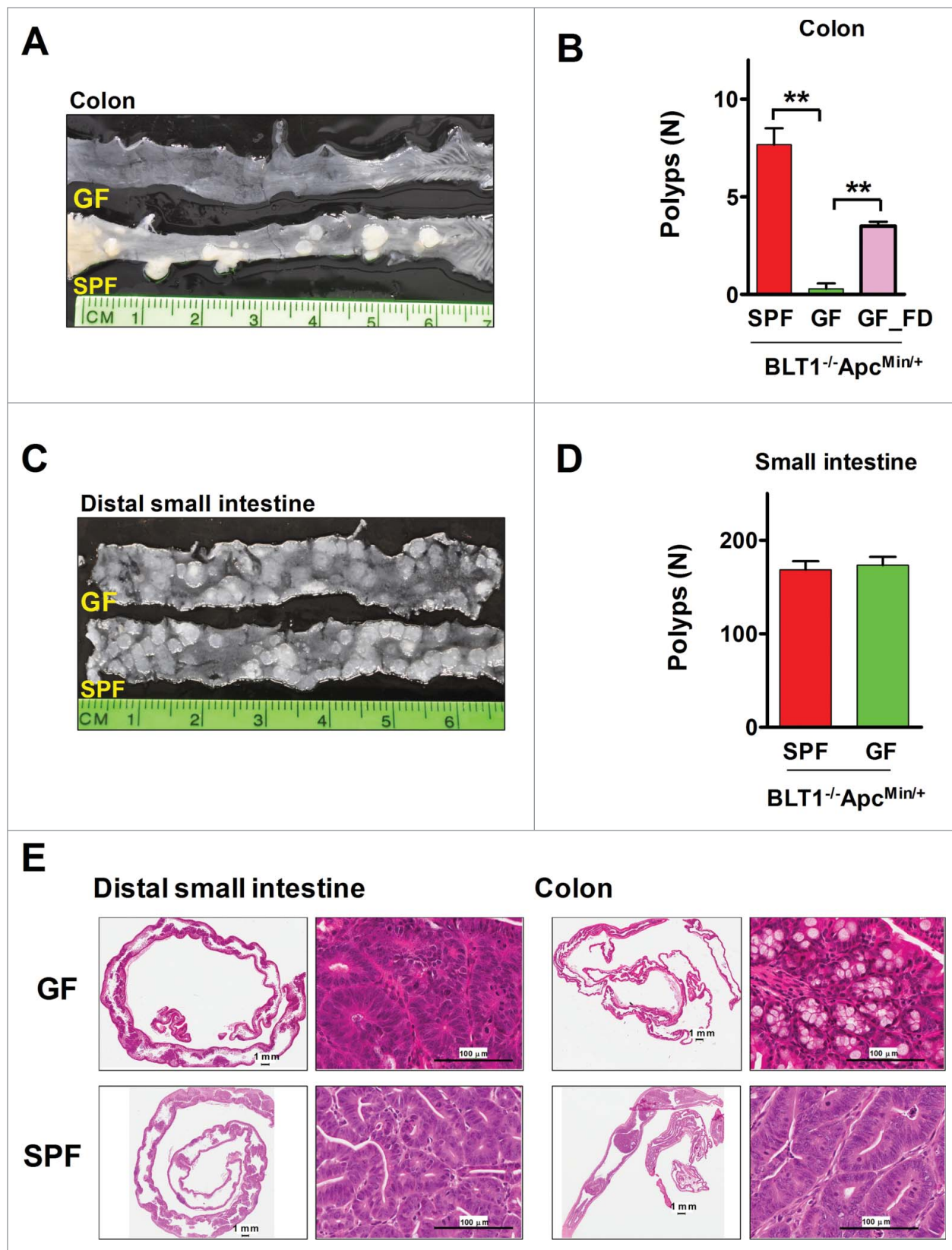


Figure 5. Germ-free BLT1^{-/-}Apc^{Min/+} mice were protected from colon cancer. (A). Gross appearance of longitudinally opened colons from BLT1^{-/-}Apc^{Min/+} mice raised and maintained in specific pathogen free (SPF) and germ free (GF) conditions. (B). BLT1^{-/-}Apc^{Min/+} mice (n = 12) maintained in germ free facility are highly protected from developing colon tumors compared with SPF facility maintained BLT1^{-/-}Apc^{Min/+} mice (n = 12). Oral gavage of fecal material from the SPF BLT1^{-/-}Apc^{Min/+} mice to germ-free BLT1^{-/-}Apc^{Min/+} mice (GF_FD; n = 8) resulted in colon tumor development in these mice. (C). Longitudinally opened distal small intestines of BLT1^{-/-}Apc^{Min/+} mice maintained specific pathogen free (SPF) or germ free (GF). (D). BLT1^{-/-}Apc^{Min/+} mice maintained in germ free or SPF facility developed similar number of small intestinal tumors. E. The representative H and E stained swiss roll sections of small intestine (distal) (left panel), colon (right panels) of the BLT1^{-/-}Apc^{Min/+} mice maintained at GF and SPF facilities. Images were captured using Aperio Image scope.

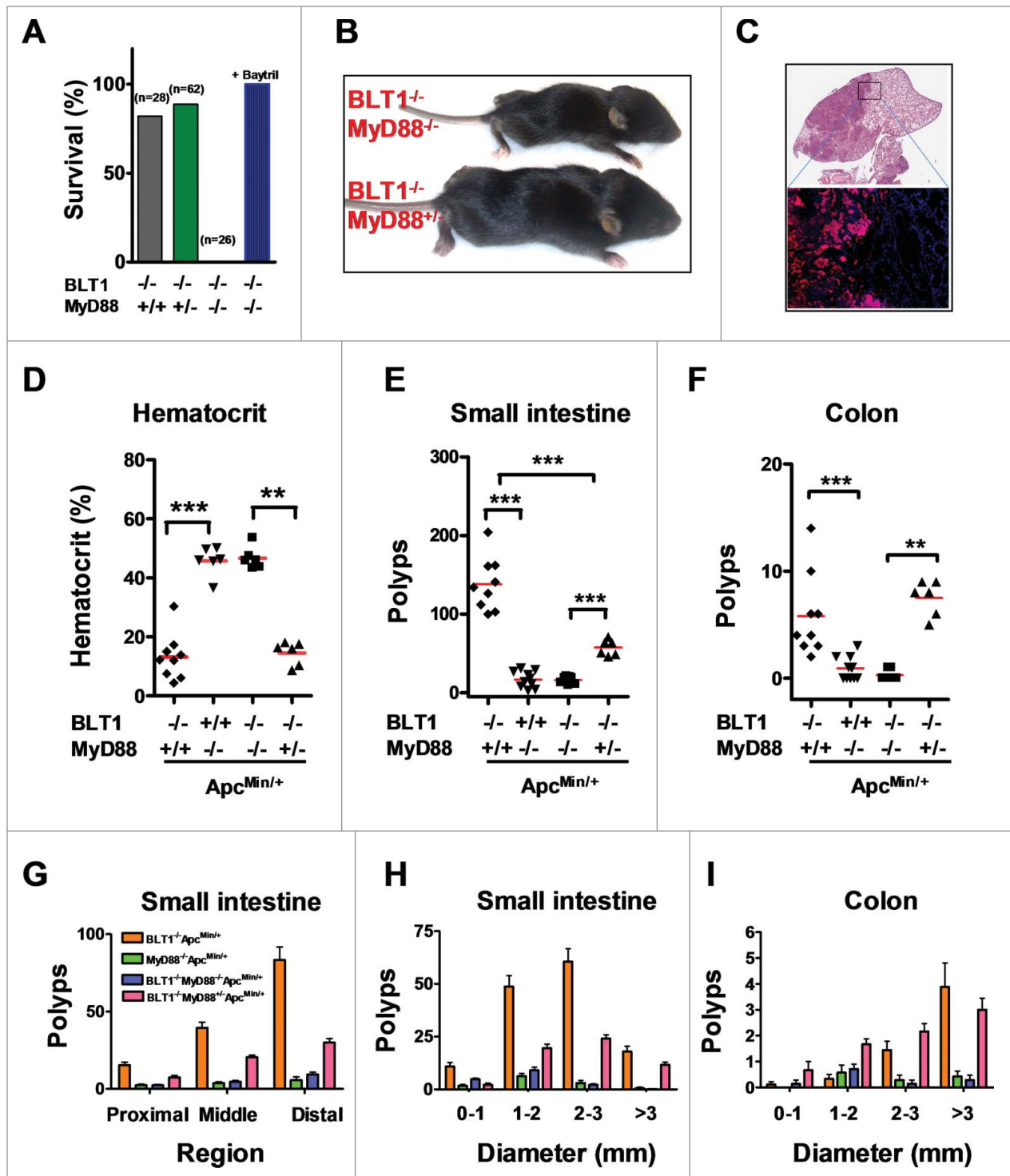


Figure 6. MyD88 acts downstream of BLT1 in promoting intestinal cancer in Apc^{Min/+} mice. (A). BLT1/MyD88 double knockout mice are susceptible to lethal neonatal infections. Percent survival of the offspring from BLT1^{-/-}MyD88^{+/-} cross (total of 15 litters from 8 different breeding pairs at day 15). Treatment of BLT1^{-/-}MyD88^{+/-} females during gestation and postpartum with a broad-spectrum antibiotic Baytril (enrofloxacin at 165 mg/L in drinking water that gave a daily dosage of ~25 mg/kg) completely reversed the early lethality of BLT1^{-/-}MyD88^{-/-} pups. (B). Double deficient (BLT1^{-/-}MyD88^{-/-}) mice are smaller compared with the littermate heterozygous mice (BLT1^{-/-}MyD88^{+/-}). (C) H&E stained cross section images of lung from (BLT1^{-/-}MyD88^{-/-} mice (top panel). The bacterial infection was detected by FISH analysis (lower panel) with Eub338-Cy3 probe (red) and nuclei of lung parenchyma stained with DAPI (blue). (D-I). The BLT1^{-/-}MyD88^{-/-}Apc^{Min/+} and littermate control animals were generated and maintained on Baytril water. The hematocrits (D), number of small intestine polyps (E) and colon polyps (F) were evaluated at 110 d age-old mice. The frequency of small intestinal tumors (G) and size ranges of tumors in both small intestine (H) and colons (I) were analyzed. The overall tumor burden in mice lacking MyD88 significantly reduced in both BLT1^{+/+} and BLT1^{-/-}Apc^{Min/+} context indicating that MyD88 acts downstream of BLT1 in promoting intestinal cancer. Statistical analysis was performed using the Mann-Whitney U test. Error bars, \pm SEM. **, $P < 0.01$; and ***, $P < 0.001$.

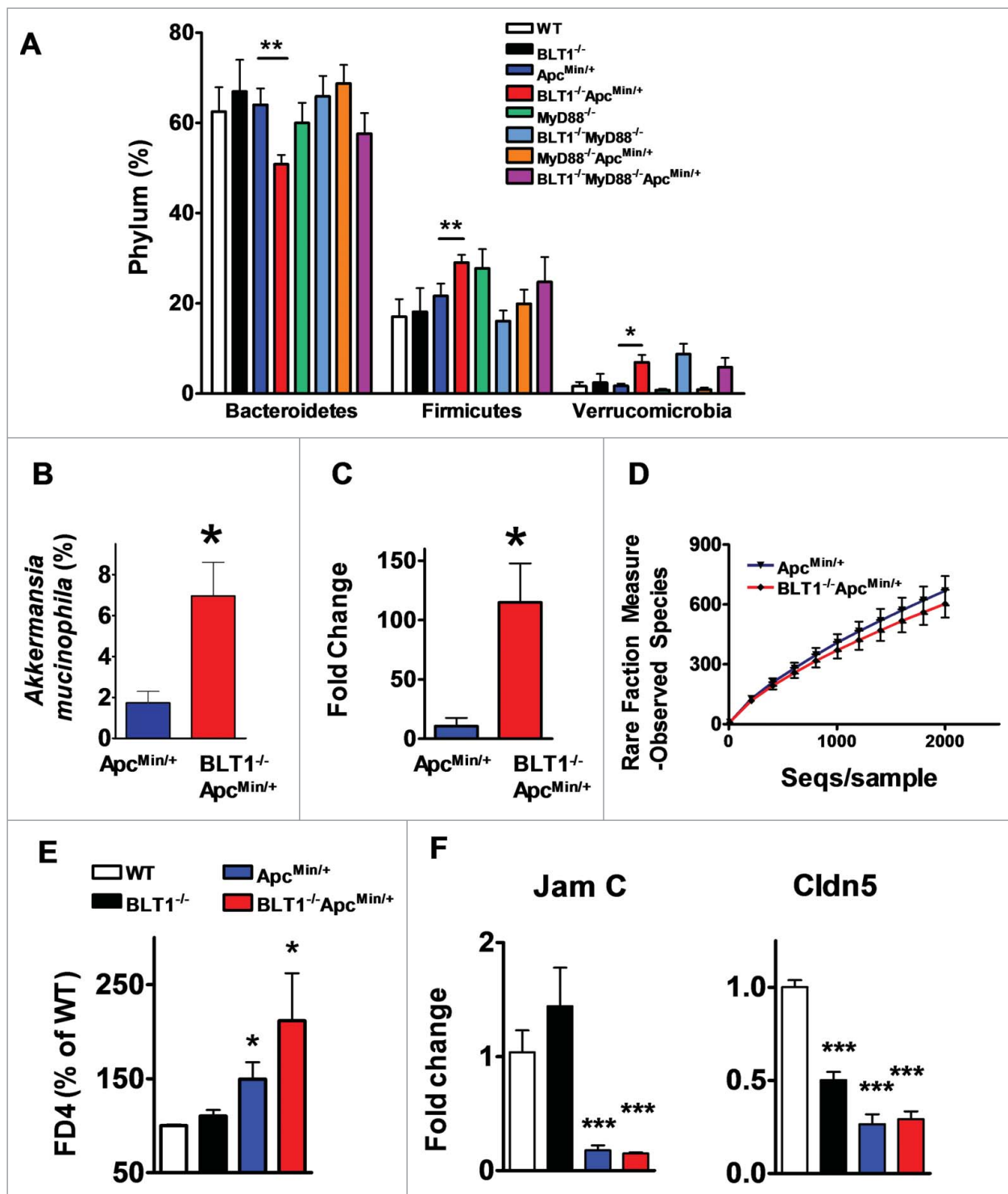


Figure 7. Modulation of gut microbiota and barrier dysfunction in BLT1^{-/-}Apc^{Min/+}. The gut microflora (fecal bacteria) was identified by sequencing 16 S rRNA gene using Roche 454 sequencer from indicated genotype (WT, n = 5; BLT1^{-/-}, n = 5; Apc^{Min/+}, n = 8; BLT1^{-/-}Apc^{Min/+}, n = 10; MyD88^{-/-}Apc^{Min/+} (n = 5); BLT1^{-/-}MyD88^{-/-}Apc^{Min/+} (n = 5)). The 16 S rRNA gene (v1-v3 regions) sequences were uploaded on to QIIME pipeline (<http://qiime.sourceforge.net/#>). The distribution of phylum (A) and genus levels (B) among genotypes were identified. Genus level analysis suggested significant increase in *Akkermansia muciniphila*. (C). The relative amounts of *Akkermansia muciniphila* from the fecal contents of indicated mice was quantified using real time PCR as described in methods. Statistical analysis performed using unpaired t-test. ** P < 0.01, *P < 0.05. (D). The α diversity is measured using qiime pipeline. (E). Increased gut permeability and decreased tight junctional proteins in tumor bearing mice. The FITC-dextran (MW_{av} = 4000; FD4) at 80 mg/mL (in 1X PBS) was administered by oral gavage (600 mg/kg bodyweight) to fasted mice. The fluorescence of FITC was measured in plasma after 2 hrs to estimate amount of FD4 leaked into blood and percent FD4 calculated using WT as base line. FD4 was significantly increased in BLT1^{-/-}Apc^{Min/+} compared with Apc^{Min/+} (*P < 0.05) and in Apc^{Min/+} compared with WT (*P < 0.05). (F). The mRNA levels of Jam C and Cldn5 were measured by RT-PCR using SyBr green. The mRNA levels were significantly reduced in tumors of Apc^{Min/+} and BLT1^{-/-}Apc^{Min/+} mice.

BLT1^{-/-}Apc^{Min/+} was further confirmed by independent assays based on real time PCR (Fig. 7C) and cloning of fecal 16 S rRNA gene amplicon and sequencing individual clones (data not shown). Interestingly, the analysis of MyD88^{-/-}Apc^{Min/+} and BLT1^{-/-}MyD88^{-/-}Apc^{Min/+} microbiota also suggested that lack of BLT1 in Apc^{Min/+} background resulted in increase in Verricomicrobia (*Akkermansia muciniphila*) (6.84% vs 0.94%) and Firmicutes (24% vs 20%) and decrease in Bacteroidetes (67% vs 58%) indicating the role for BLT1 in MyD88 independent manner to modulate the gut flora in Apc^{Min/+} mice (Fig. 7A). It is important to note that even in the absence of Apc^{Min/+} mutation in BLT1^{-/-}MyD88^{-/-} mice showed an increase in *Akkermansia* suggesting that the BLT1 and MyD88 synergistically control the *Akkermansia*. However, in the context of Apc^{Min/+} mutation, lack of BLT1 alone is sufficient to allow the outgrowth of *Akkermansia*. The α rare fraction analysis of observed species among Apc^{Min/+} and BLT1^{-/-}Apc^{Min/+} shows distinct genotype associated differences between the groups (Fig. 7D).

Adenoma induced barrier dysfunction is a major contributor to the progression of colon tumors in Apc^{Min/+} models.⁵² Barrier dysfunction leading to intestinal permeability was measured in dextran-FITC fed mice. As shown in Fig. 7E, the mice in Apc^{Min/+} background (both BLT1^{-/-}Apc^{Min/+} and BLT1^{+/+}Apc^{Min/+}) showed increased intestinal leakage of dextran FITC into blood compared with non-cancerous mice suggesting damage of intestinal barrier in tumor bearing mice. The leakage of dextran-FITC is significantly more in BLT1^{-/-}Apc^{Min/+} mice possibly due to increased tumor burden. The expression analysis of junctional proteins revealed a significant reduction in Cldn5 and Jam-C mRNA expression in colon tumors compared with normal colon (Fig. 7F). These results suggest that adenoma induced barrier dysfunction likely forms the basis for host genotype dependent reshaping of microbiota (Fig. 7A).

Discussion

Leukotriene B₄ and its receptors have been a major focus in diverse inflammatory diseases over the past 2 decades. An emerging view from these studies is that inflammation promoted by the high affinity LTB₄ receptor BLT1 is detrimental and is coincidental with the development and progression of asthma,²⁸ arthritis,^{29,30} atherosclerosis²⁷ and lung cancers.⁵³ The results presented here outline a beneficial role for BLT1-mediated inflammation in host response to mucosal infections and control of spontaneous intestinal tumor development in Apc^{Min/+} mice.

In the Apc^{Min/+} mice most adenomas develop in the small intestine.²¹ This is in contrast to *Apc* mutations in humans that invariably lead to colon tumor development. The BLT1^{-/-}Apc^{Min/+} model described in this study, while retaining the small intestine specificity of the mouse Apc^{Min/+}, develops very large multiple colonic adenomas reminiscent of human colon cancers. This phenotype retains the requirement for early mutations in the *APC* gene as the BLT1^{-/-} mice do not develop any spontaneous tumors in colon. Previous studies have shown that regulators of the eicosanoid pathways such as cPLA2, COX2 and

prostaglandin E2 receptor (EP2) to be tumor promoting in Apc^{Min/+} mice,⁵⁴⁻⁵⁷ but the role of LTB₄/BLT1 pathway was unknown. Use of dual 5-LOX/COX inhibitor, licoferone reduced the overall tumorigenesis in Apc^{Min/+} mouse model suggesting importance of leukotriene pathway in tumor development.⁵⁸ In support of this observation, 5-LO^{-/-} in APC^{Δ468} background led to a dramatic reduction in the number and size of intestinal polyps.⁵⁹ It was suggested that haematopoietic expression (mast cells) of 5-LO is critical in recruitment of myeloid-derived suppressor cells (MDSCs) to promote tumorigenesis in this model.⁵⁹ We also generated 5LO^{-/-}Apc^{Min/+} compound mice in our laboratory and evaluated the survival of mice. The deficiency of 5-LO increased the survival of Apc^{Min/+} mice as well as reduced their anemic status (Supplementary Figure 7A and B). Importantly, 5LO^{-/-}Apc^{Min/+} displayed decreased polyps number (Supplementary Figure 7C) suggesting that 5-LO might play a role in tumor initiation corroborating with phenotype of 5-LO^{-/-}APC^{Δ468}. Thus, 5-LO derived products other than LTB₄ could have a direct promotional activity on intestinal tumors. In this context, cystinyl leukotriene receptor 1 (CysLT1) deficient mice in the Apc^{Min/+} background were shown to display reduced tumor burden.⁶⁰ Previously, Dreyling *et al.* showed that LTB₄ levels are significantly increased in human gastrointestinal adenocarcinoma compared with normal colonic mucosa.⁶¹ In Apc^{Min/+} mice, it was demonstrated that small intestinal tumors produced significantly higher levels of LTB₄.⁶² Mucosal mast cells might be the initial source of LTB₄ that recruit additional LTB₄ producing (granulocytes) cells involved in host response to infections.

The unexpected observations made in this study with BLT1^{-/-} mice suggests that LTB₄ pathway protects Apc^{Min/+} mice from developing intestinal tumors. Several lines of evidence point to an important role for BLT1 in host response to infection. The decrease in multiple antibacterial proteins at the mucosal surfaces and in intestinal tumors in BLT1^{-/-}Apc^{Min/+} mice as well as decreased neutrophils influx and increased bacterial loads in response to peritoneal *E. coli* infection (Supplementary Figure 8) suggests that BLT1 is a mediator of host response to infection. These observations are consistent with the earlier findings that LTB₄ directly activates production of β -defensins^{63,64} as well as decreased inflammatory cell influx in a model of septic peritonitis.⁶⁵ Addition of LTB₄ was also shown to increase in bactericidal activity of alveolar macrophages from 5-lipoxygenase deficient mice.⁶⁶ The increased susceptibility to DSS induced colitis and increased bacterial load in BLT1^{-/-} mice also support the notion that BLT1 is a critical mediator of host defense mechanisms. The protective role of BLT1 in colon tumor progression is also evident in the AOM-DSS induced colon cancer in mice (Fig. 3).

The complete absence of colon tumors in germ-free BLT1^{-/-}Apc^{Min/+} mice and their reappearance upon fecal transplantation from SPF BLT1^{-/-}Apc^{Min/+} mice suggests that microbiota induced inflammation is a critical step in the development of spontaneous colon tumors. Interestingly, small intestinal tumor progression in BLT1^{-/-}Apc^{Min/+} mice is bacteria independent as evident from unaltered tumor burden in germ free mice (Fig. 5) that may be controlled by immune surveillance

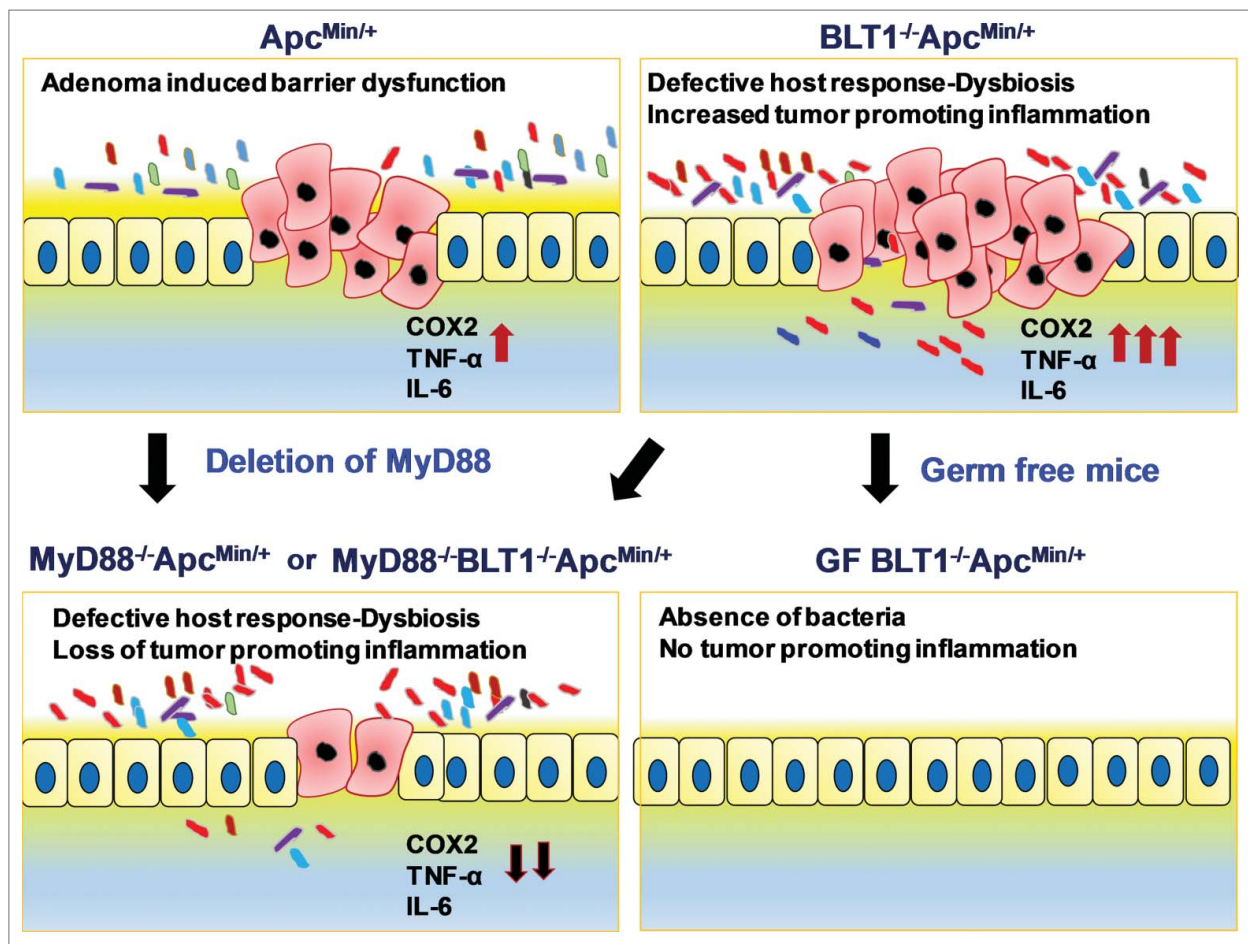


Figure 8. Interplay of BLT1 and MyD88 Signaling in Intestinal tumor development: Adenoma induced barrier dysfunction in $Apc^{Min/+}$ mice induces tumor promoting inflammation. Absence of BLT1 amplifies tumor initiated microbial dysbiosis leading to both bacteria (germ-free) and MyD88 dependent inflammation that promotes tumor progression.

mechanisms. In this regard, we recently demonstrated using transplantable cervical cancer (TC1) and B16 melanoma models that expression of BLT1 on $CD8^+$ T-cells is required for their migration into tumors to elicit effective anti-tumor immunity.^{67,68} In these models, we showed accelerated tumor growth and decreased survival in $BLT1^{-/-}$ mice compared with wild type mice. T cell depletion and adoptive transfer of CTLs into $Rag2^{-/-}$ mice showed requirement for BLT1 on $CD8^+$ T cells for effective immune surveillance. Numerous studies with human cancers showed a strong correlation between $CD8^+$ T cell infiltration and long-term survival.⁶⁹ Our studies highlighted the critical nature of BLT1/LTB₄ axis in the process of CTL recruitment to the sites of tumors for effective immune surveillance.

The current studies have uncovered a synergy between TLR-mediated inflammation and BLT1 mediated antibacterial response as seen by the lethal neonatal sepsis in $BLT1/MyD88$ double deficient mice. MyD88 was shown to directly influence the gut flora and these alterations have direct consequence to disease development.⁷⁰ The significant decrease in tumorigenesis in $BLT1^{-/-}MyD88^{-/-}Apc^{Min/+}$ suggests that BLT1 acts upstream of MyD88 promoted inflammation in colon tumorigenesis. A single copy of MyD88 gene is sufficient to promote tumor growth in $Apc^{Min/+}$ model (Fig. 6E-G) indicating the

critical nature of MyD88 signaling cascade in tumor progression. Absence of MyD88 is highly protective in the small intestinal tumor despite lack of immune surveillance mechanisms mediated by BLT1 ($BLT1^{-/-}MyD88^{-/-}Apc^{Min/+}$) suggesting a critical role for MyD88 in intestinal epithelial cell (IECs) proliferation apart from its classical role in host-defense mechanisms. In this regard, it was demonstrated that non-haematopoietic cells, such as IECs, required MyD88 for intestinal tumor growth.⁷¹ It was suggested that TLR ligands derived from microbiota mediate the IEC tumor growth through ERK activation by stabilizing/increasing abundance of Myc protein, the product of oncogene c-Myc. Interestingly, our studies demonstrate that germ-free $BLT1^{-/-}Apc^{Min/+}$ mice did not alter the small intestinal tumor growth suggesting, bacterial independent, but MyD88 dependent tumor growth through yet unknown mechanisms. In contrast to spontaneous intestinal tumor model, deficiency of MyD88 in AOM-DSS induced colon tumor model significantly increased the colon tumor burden.⁷² However, it is possible that extensive breach in the intestinal barrier caused by DSS could lead to leaky gut and bacteria, which will not be cleared in $MyD88^{-/-}$ mice leading to significantly increased inflammation associated colon tumors.

Microbiota is known to play a critical role in modulating the both innate and adaptive immune systems as well as

regulate various disease conditions.⁷³⁻⁸⁰ Our analysis of the 16 S rRNA gene sequences from fecal material of *Apc*^{Min/+} and *BLT1*^{-/-}*Apc*^{Min/+} showed major and distinct differences with an increase in *Akkermansia muciniphila* in *BLT1*^{-/-}*Apc*^{Min/+} compared with *Apc*^{Min/+} mice. *A. muciniphila* (belongs to Verrucomicrobia phylum) is known as a mucin degrading bacteria present in the human intestines.⁸¹⁻⁸³ *A. muciniphila* represented a relatively large percentage of sequences in human fecal microbiota of colon cancer patients,⁸⁴ ulcerative colitis-associated pouchitis⁸⁵ compared with healthy people. Mucin acts as a protective barrier between the intestinal contents and the mucosal wall and it is possible that enhanced degradation of mucin in *BLT1*^{-/-}*Apc*^{Min/+} makes the intestines more permeable to pathogenic bacteria resulting in increased inflammation. Consistent with this notion, studies showed that a mucin deficient *Apc*^{Min/+} mice (*Muc2*^{-/-}*Apc*^{Min/+}) develop significant colon tumor burden.⁸⁶ Additional subtype taxonomy analysis (Supplementary Fig. 9) revealed that bacteria belonging to family S24-7 (Bacteroidetes phylum) are significantly downregulated in *BLT1*^{-/-}*Apc*^{Min/+} mice. But absence of *MyD88*^{-/-} in this context did not alter the bacterial populations of S24-7. Most interestingly, *Prevotella* and bacteria belonging to *Rikenellaceae* are absent in mice lacking of *MyD88* independent of *Apc*^{Min/+} mutation. The importance of these findings require additional studies. It is interesting to note that increase in *A. muciniphila* is *BLT1* dependent (in context of either *MyD88*^{-/-} or *Apc*^{Min/+} background), but requires *MyD88* to promote colon tumorigenesis. The most significant observation of the current studies is the direct link between the altered microbiome in *BLT1* deficient mice to increased *MyD88* dependent inflammation in the intestinal tumors in the *BLT1*^{-/-}*Apc*^{Min/+} mice.

Defective expression of tight junctional proteins (intestinal barrier proteins) such as JAM-A, JAM-B was an early event in colorectal cancer tumorigenesis followed by upregulation of IL-23 and IL-17 by microbial products to promote inflammation mediated colorectal cancer.⁵² Our results also suggests that decreased expression of the junctional proteins (*Cldn5* and JAM-C) and increased intestinal permeability in mice harbouring *Apc*^{Min/+} mutation. Defective host response in combination with increased intestinal permeability in *BLT1*^{-/-}*Apc*^{Min/+} mice likely resulted in reshaping of the gut microbiota leading to increased inflammation and tumorigenesis. Further studies are needed to define the role of individual bacteria in promoting colon tumors.

These results suggest an intricate interplay of host response and inflammation in tumor development (Fig. 8). Adenoma induced barrier dysfunction in *Apc*^{Min/+} mice initiates epithelial breach and induces inflammation. Absence of *BLT1* in colon alters the host response reshaping the gut microbiota and sets up conditions for enhanced chronic inflammation and tumor promotion. The ensuing microbial dysbiosis amplifies bacteria induced colonic inflammation primarily through activation of a set of bacterial 'sensors' exemplified by the typical TLR pathways that mobilize a group of 'mediators' such as the IL-6 and inflammatory chemokines to clear these mucosal infections.⁸⁷ Under germ-free conditions or in the absence of *MyD88*, loss of bacteria induced inflammation prevents tumor progression. Our results highlight the importance of *BLT1* mediated early

inflammation in reducing dysbiosis, the underlying cause of gut inflammation and protecting from colon tumor development.

Acknowledgments

We thank Dr. Nejat Egilmez for critical reading of the manuscript. We thank Haritha Pallam and Michelle Smith for expert technical assistance. We thank Luke Ursell from Rob Knight's group in setting up the microbiota analysis. This work was supported by NIH grants CA-138623(BH) and James Graham Brown Cancer Center at U of L. Part of this work was performed with assistance of the U of L Microarray Facility, which is supported by NCRN COBRE P20RR018733, KY-INBRE NCRN P20RR016481 and the J. G. Brown Cancer Center at U of L. The authors declare no competing financial interests.

Author contributions

V.R.J., and P.M., contributed equally to this work; V.R.J., and B.H. designed research; P.M., E.K. and V.R.J., S.R.B., M.W., S.M., K.S. performed research; A.B.J., M.L.P., E.R. and R.N. contributed analytic tools; P.M., V.R.J., and B.H. analyzed data; and V.R.J., S.R.B. and B.H. wrote the paper.

ORCID

Eric C. Rouchka  <http://orcid.org/0000-0003-3487-6572>

References

- Coussens LM, Werb Z. Inflammation and cancer. *Nature*. 2002;420:860-867. doi:10.1038/nature01322
- Karin M, Lawrence T, Nizet V. Innate immunity gone awry: linking microbial infections to chronic inflammation and cancer. *Cell*. 2006;124:823-835. doi:10.1016/j.cell.2006.02.016. PMID:16497591
- Mantovani A, Allavena P, Sica A, Balkwill F. Cancer-related inflammation. *Nature*. 2008;454:436-444. doi:10.1038/nature07205. PMID:18650914
- Greten FR, Eckmann L, Greten TF, Park JM, Li ZW, Egan LJ, Kagnoff MF, Karin M. IKKbeta links inflammation and tumorigenesis in a mouse model of colitis-associated cancer. *Cell*. 2004;118, 285-296. doi:10.1016/j.cell.2004.07.013. PMID:15294155
- Dzutsev A, Goldszmid RS, Viaud S, Zitvogel L, Trinchieri G. The role of the microbiota in inflammation, carcinogenesis, and cancer therapy. *European Journal of Immunology*. 2015;45:17-31. doi:10.1002/eji.201444972. PMID:25328099
- Roy S, Trinchieri G. Microbiota: a key orchestrator of cancer therapy. *Nature Reviews Cancer*. 2017;17(5):271-285. doi:10.1038/nrc.2017.13. PMID:28303904
- Neish AS. Microbes in gastrointestinal health and disease. *Gastroenterology*. 2009;136:65-80. doi:10.1053/j.gastro.2008.10.080. PMID:19026645
- Sobhani I, Tap J, Roudot-Thoraval F, Roperch JP, Letulle S, Langella P, Corthier G, Tran Van Nhieu J, Furet JP, et al. Microbial dysbiosis in colorectal cancer (CRC) patients. *PloS One*. 2011;6:e16393. doi:10.1371/journal.pone.0016393. PMID:21297998
- Schwabe RF, Jobin C. The microbiome and cancer. *Nature Reviews Cancer*. 2013;13:800-812. doi:10.1038/nrc3610. PMID:24132111
- Vipperla K, O'Keefe SJ. The microbiota and its metabolites in colonic mucosal health and cancer risk. *Nutrition in Clinical Practice: Official Publication of the American Society for Parenteral and Enteral Nutrition*. 2012;27:624-635. doi:10.1177/0885433612452012. PMID:22868282
- Waisberg J, Matheus Cde O, Pimenta J. Infectious endocarditis from *Streptococcus bovis* associated with colonic carcinoma: case report and literature review. *Arq Gastroenterol*. 2002;39:177-180. PMID:12778310
- Gold JS, Bayar S, Salem RR. Association of *Streptococcus bovis* bacteremia with colonic neoplasia and extracolonic malignancy. *Arch Surg*. 2004;139:760-765. doi:10.1001/archsurg.139.7.760. PMID:15249410

13. Klein RS, Recco RA, Catalano MT, Edberg SC, Casey JI, Steigbigel NH. Association of *Streptococcus bovis* with carcinoma of the colon. *N Engl J Med*. 1977;297:800-802. doi:10.1056/NEJM197710132971503. PMID:408687
14. Zarkin BA, Lillemoe KD, Cameron JL, Effron PN, Magnuson TH, Pitt HA. The triad of *Streptococcus bovis* bacteremia, colonic pathology, and liver disease. *Ann Surg*. 1990;211:786-791; discussion 791-782. PMID:2357141
15. Ruoff KL, Miller SI, Garner CV, Ferraro MJ, Calderwood SB. Bacteremia with *Streptococcus bovis* and *Streptococcus salivarius*: clinical correlates of more accurate identification of isolates. *J Clin Microbiol* 1989;27:305-308 PMID:2915024
16. Tsuji S, Tsujii M, Murata H, Nishida T, Komori M, Yasumaru M, Ishii S, Sasayama Y, Kawano S, Hayashi N. *Helicobacter pylori* eradication to prevent gastric cancer: underlying molecular and cellular mechanisms. *World J Gastroenterol*. 2006;12:1671-1680. PMID:16586533
17. Huang JQ, Zheng GF, Sumanak K, Irvine EJ, Hunt RH. Meta-analysis of the relationship between cagA seropositivity and gastric cancer. *Gastroenterology*. 2003;125:1636-1644. PMID:14724815
18. Martin HM, Campbell BJ, Hart CA, Mpofu C, Nayar M, Singh R, Englyst H, Williams HF, Rhodes JM. Enhanced *Escherichia coli* adherence and invasion in Crohn's disease and colon cancer. *Gastroenterology*. 2004;127:80-93. PMID:15236175
19. Chen W, Liu F, Ling Z, Tong X, Xiang C. Human intestinal lumen and mucosa-associated microbiota in patients with colorectal cancer. *PloS One*. 2012;7:e39743. doi:10.1371/journal.pone.0039743. PMID:22761885
20. Aoki K, Taketo MM. Adenomatous polyposis coli (APC): a multifunctional tumor suppressor gene. *J Cell Sci*. 2007;120:3327-3335. doi:10.1242/jcs.03485. PMID:17881494
21. Moser AR, Pitot HC, Dove WF. A dominant mutation that predisposes to multiple intestinal neoplasia in the mouse. *Science*. 1990;247:322-324. PMID:2296722
22. Rakoff-Nahoum S, Medzhitov R. Regulation of spontaneous intestinal tumorigenesis through the adaptor protein MyD88. *Science*. 2007;317:124-127. doi:10.1126/science.1140488. PMID:17615359
23. Toda A, Yokomizo T, Shimizu T. Leukotriene B4 receptors. *Prostaglandins & Other Lipid Mediators*. 2002;68-69:575-585.
24. Yokomizo T, Izumi T, Chang K, Takuwa Y, Shimizu T. A G-protein-coupled receptor for leukotriene B4 that mediates chemotaxis. *Nature*. 1997;387:620-624. doi:10.1038/42506. PMID:9177352
25. Yokomizo T, Kato K, Terawaki K, Izumi T, Shimizu T. A second leukotriene B(4) receptor, BLT2. A new therapeutic target in inflammation and immunological disorders. *The Journal of Experimental Medicine*. 2000;192:421-432. PMID:10934230
26. Tager AM, Bromley SK, Medoff BD, Islam SA, Bercury SD, Friedrich EB, Carafone AD, Gerszten RE, Luster AD. Leukotriene B4 receptor BLT1 mediates early effector T cell recruitment. *Nature Immunology*. 2003;4:982-990. doi:10.1038/nri970. PMID:12949531
27. Subbarao K, Jala VR, Mathis S, Suttles J, Zacharias W, Ahamed J, Ali H, Tseng MT, Haribabu B. Role of leukotriene B4 receptors in the development of atherosclerosis: potential mechanisms. *Arterioscler Thromb Vasc Biol*. 2004;24:369-375. doi:10.1161/01.ATV.0000110503.16605.15. PMID:14656734
28. Miyahara N, Takeda K, Miyahara S, Matsubara S, Koya T, Joetham A, Krishnan E, Dakhama A, Haribabu B, Gelfand EW. Requirement for leukotriene B4 receptor 1 in allergen-induced airway hyperresponsiveness. *American Journal Of Respiratory And Critical Care Medicine*. 2005;172:161-167. doi:10.1164/rccm.200502-205OC. PMID:15849325
29. Kim ND, Chou RC, Seung E, Tager AM, Luster AD. A unique requirement for the leukotriene B4 receptor BLT1 for neutrophil recruitment in inflammatory arthritis. *The Journal of Experimental Medicine*. 2006;203:829-835. doi:10.1084/jem.20052349. PMID:16567386
30. Shao WH, Del Prete A, Bock CB, Haribabu B. Targeted disruption of leukotriene B4 receptors BLT1 and BLT2: a critical role for BLT1 in collagen-induced arthritis in mice. *Journal of Immunology*. 2006;176:6254-6261.
31. Houthuijzen JM, Daenen LG, Roodhart JM, Oosterom I, van Jaarsveld MT, Govaert KM, Smith ME, Sadatmand SJ, Rosing H, Kruse F, et al. Lysophospholipids secreted by splenic macrophages induce chemotherapy resistance via interference with the DNA damage response. *Nat Commun*. 2014;5:5275. doi:10.1038/ncomms6275. PMID:25387467
32. Haribabu B, Verghese MW, Steeber DA, Sellars DD, Bock CB, Snyderman R. Targeted disruption of the leukotriene B(4) receptor in mice reveals its role in inflammation and platelet-activating factor-induced anaphylaxis. *J Exp Med*. 2000;192:433-438. PMID:10934231
33. Marr KA, Balajee SA, Hawn TR, Ozinsky A, Pham U, Akira S, Aderem A, Liles WC. Differential role of MyD88 in macrophage-mediated responses to opportunistic fungal pathogens. *Infect Immun*. 2003;71:5280-5286. PMID:12933875
34. Caporaso JG, Kuczynski J, Stombaugh J, Bittinger K, Bushman FD, Costello EK, Fierer N, Peña AG, Goodrich JK, Gordon JI, et al. QIIME allows analysis of high-throughput community sequencing data. *Nature Methods*. 2010;7:335-336. doi:10.1038/nmeth.f.303. PMID:20383131
35. Lozupone C, Lladser ME, Knights D, Stombaugh J, Knight R. UniFrac: an effective distance metric for microbial community comparison. *The ISME Journal* 2011;5:169-172. doi:10.1038/ismej.2010.133. PMID:20827291
36. Livak KJ, Schmittgen TD. Analysis of relative gene expression data using real-time quantitative PCR and the 2(-Delta Delta C(T)) method. *Methods*. 2001;25:402-408. doi:10.1006/meth.2001.1262. PMID:11846609
37. Kinzler KW, Vogelstein B. Lessons from hereditary colorectal cancer. *Cell*. 1996;87:159-170. PMID:8861899
38. Humphries A, Wright NA. Colonic crypt organization and tumorigenesis. *Nat Rev Cancer*. 2008;8:415-424. doi:10.1038/nrc2392. PMID:18480839
39. Karin M, Greten FR. NF-kappaB: linking inflammation and immunity to cancer development and progression. *Nat Rev Immunol*. 2005;5:749-759. doi:10.1038/nri1703. PMID:16175180
40. Williams CS, et al. Elevated cyclooxygenase-2 levels in Min mouse adenomas. *Gastroenterology*. 1996;111:1134-1140. doi:S0016-5085(96)70083-5. PMID:8831610
41. Carlin JM, Borden EC, Byrne GI. Interferon-induced indoleamine 2,3-dioxygenase activity inhibits *Chlamydia psittaci* replication in human macrophages. *J Interferon Res* 1989;9:329-337. PMID:2501398
42. Thomas SM, Garrity LF, Brandt CR, Schobert CS, Feng GS, Taylor MW, Carlin JM, Byrne GI. IFN-gamma-mediated antimicrobial response. Indoleamine 2,3-dioxygenase-deficient mutant host cells no longer inhibit intracellular *Chlamydia* spp. or *Toxoplasma* growth. *J Immunol*. 1993;150:5529-5534 PMID:8515074
43. Hooper LV, Stappenbeck TS, Hong CV, Gordon JI. Angiogenins: a new class of microbicidal proteins involved in innate immunity. *Nat Immunol*. 2003;4:269-273. doi:10.1038/ni888ni888. PMID:12548285
44. Boix E, Nogues MV. Mammalian antimicrobial proteins and peptides: overview on the RNase A superfamily members involved in innate host defence. *Mol Biosyst*. 2007;3:317-335. doi:10.1039/b617527a. PMID:17460791
45. Rosenberg HF. RNase A ribonucleases and host defense: an evolving story. *J Leukoc Biol*. 2008;83:1079-1087. doi:10.1189/jlb.1107725. PMID:18211964
46. Cash HL, Whitham CV, Behrendt CL, Hooper LV. Symbiotic bacteria direct expression of an intestinal bactericidal lectin. *Science*. 2006;313:1126-1130. doi:10.1126/science.1127119. PMID:16931762
47. Soares EM, Mason KL, Rogers LM, Serezani CH, Faccioli LH, Aronoff DM. Leukotriene B4 enhances innate immune defense against the periperal sepsis agent *Streptococcus pyogenes*. *Journal of Immunology*. 2013;190:1614-1622. doi:10.4049/jimmunol.1202932
48. Sorgi CA, Secatto A, Fontanari C, Turato WM, Belang er C, de Medeiros AI, Kashima S, Marleau S, Covas DT, Bozza PT, et al. Histoplasma capsulatum cell wall [beta]-glucan induces lipid body formation through CD18, TLR2, and dectin-1 receptors: correlation with leukotriene B4 generation and role in HIV-1 infection. *Journal of Immunology*. 2009;182:4025-4035. doi:10.4049/jimmunol.0801795
49. Gaudreault E, Gosselin J. Leukotriene B4-mediated release of antimicrobial peptides against cytomegalovirus is BLT1 dependent. *Viral Immunology*. 2007;20:407-420. doi:10.1089/vim.2006.0099. PMID:17931111
50. Serezani CH, Perrela JH, Russo M, Peters-Golden M, Jancar S. Leukotrienes are essential for the control of *Leishmania amazonensis*

- infection and contribute to strain variation in susceptibility. *Journal Of Immunology*. 2006;177:3201-3208.
51. Naugler WE, Sakurai T, Kim S, Maeda S, Kim K, Elsharkawy AM, Karin M. Gender disparity in liver cancer due to sex differences in MyD88-dependent IL-6 production. *Science*. 2007;317:121-124. doi:10.1126/science.1140485. PMID:17615358
 52. Grivennikov SI, Wang K, Mucida D, Stewart CA, Schnabl B, Jauch D, Taniguchi K, Yu GY, Osterreicher CH, Hung K, et al. Adenoma-linked barrier defects and microbial products drive IL-23/IL-17-mediated tumour growth. *Nature*. 2012;491:254-258. doi:10.1038/nature11465 PMID:23034650
 53. Satpathy SR, Jala VR, Bodduluri SR, Krishnan E, Hegde B, Hoyle GW, Fraig M, Luster AD, Haribabu B. Crystalline silica-induced leukotriene B4-dependent inflammation promotes lung tumour growth. *Nat Commun*. 2015;6:7064. doi:10.1038/ncomms8064. PMID:25923988
 54. Hong KH, Bonventre JC, O'Leary E, Bonventre JV, Lander ES. Deletion of cytosolic phospholipase A(2) suppresses Apc(Min)-induced tumorigenesis. *Proc Natl Acad Sci U S A*. 2001;98:3935-3939. doi:10.1073/pnas.051635898. PMID:11274413
 55. Kawai N, Tsujii M, Tsuji S. Cyclooxygenases and colon cancer. *Prostaglandins & Other Lipid Mediators*. 2002;68-69:187-196.
 56. Wang D, Wang H, Shi Q, Katkuri S, Walhi W, Desvergne B, Das SK, Dey SK, DuBois RN. Prostaglandin E(2) promotes colorectal adenoma growth via transactivation of the nuclear peroxisome proliferator-activated receptor delta. *Cancer Cell*. 2004;6:285-295. doi:10.1016/j.ccr.2004.08.011. PMID:15380519
 57. Oshima M, Dinchuk JE, Kargman SL, Oshima H, Hancock B, Kwong E, Trzaskos JM, Evans JF, Taketo MM. Suppression of intestinal polyposis in Apc delta716 knockout mice by inhibition of cyclooxygenase 2 (COX-2). *Cell*. 1996;87:803-809. doi:S0092-8674(00)81988-1. PMID:8945508
 58. Mohammed A, Janakiram NB, Li Q, Choi CI, Zhang Y, Steele VE, Rao CV. Chemoprevention of colon and small intestinal tumorigenesis in APC(Min/+) mice by licoferone, a novel dual 5-LOX/COX inhibitor: potential implications for human colon cancer prevention. *Cancer Prevention Research*. 2011;4:2015-2026. doi:10.1158/1940-6207.CAPR-11-0233. PMID:21885812
 59. Cheon EC, Khazaie K, Khan MW, Strouch MJ, Krantz SB, Phillips J, Blatner NR, Hix LM, Zhang M, Dennis KL, et al. Mast cell 5-lipoxygenase activity promotes intestinal polyposis in APCDelta468 mice. *Cancer Research*. 2011;71:1627-1636. doi:10.1158/0008-5472.CAN-10-1923. PMID:21216893
 60. Mehdawi L, Osman J, Topi G, Sjolander A. High tumor mast cell density is associated with longer survival of colon cancer patients. *Acta Oncol*. 2016;55:1434-1442. doi:10.1080/0284186X.2016.1198493. PMID:27355473
 61. Dreyling KW, Hoppe U, Peskar BA, Morgenroth K, Kozushek W, Peskar BM. Leukotriene synthesis by human gastrointestinal tissues. *Biochim Biophys Acta*. 1986;878:184-193. PMID:3019409
 62. Chiu CH, McEntee MF, Whelan J. Sulindac causes rapid regression of preexisting tumors in Min/+ mice independent of prostaglandin biosynthesis. *Cancer Research*. 1997;57:4267-4273. PMID:9331087
 63. Flamand L, Tremblay MJ, Borgeat P. Leukotriene B4 triggers the in vitro and in vivo release of potent antimicrobial agents. *Journal of Immunology*. 2007;178:8036-8045. doi:178/12/8036
 64. Gaudreault E, Gosselin J. Leukotriene B4 induces release of antimicrobial peptides in lungs of virally infected mice. *Journal of Immunology* 2008;180:6211-6221. doi:180/9/6211
 65. Scott MJ, Cheadle WG, Hoth JJ, Peyton JC, Subbarao K, Shao WH, Haribabu B. Leukotriene B4 receptor (BLT-1) modulates neutrophil influx into the peritoneum but not the lung and liver during surgically induced bacterial peritonitis in mice. *Clinical and Diagnostic Laboratory Immunology*. 2004;11:936-941. doi:10.1128/CDLI.11.5.936-941.2004. PMID:15358656
 66. Mancuso P, Standiford TJ, Marshall T, Peters-Golden M. 5-Lipoxygenase reaction products modulate alveolar macrophage phagocytosis of *Klebsiella pneumoniae*. *Infect Immun*. 1998;66:5140-5146. PMID:9784515
 67. Sharma RK, Chheda Z, Jala VR, Haribabu B. Expression of Leukotriene B4 Receptor-1 on CD8+ T Cells is required for their migration into tumors to elicit effective antitumor immunity. *Journal of Immunology* 2013;191:3462-3470. doi:10.4049/jimmunol.1300967
 68. Chheda ZS, Sharma RK, Jala VR, Luster AD, Haribabu B. Chemoattractant receptors BLT1 and CXCR3 regulate antitumor immunity by facilitating CD8+ T Cell migration into tumors. *J Immunol*. 2016;197:2016-2026. doi:10.4049/jimmunol.1502376. PMID:27465528
 69. Bindea G, Mlecnik B, Tosolini M, Kirilovsky A, Waldner M, Obenauf AC, Angell H, Fredriksen T, Lafontaine L, Berger A, et al. Spatiotemporal dynamics of intratumoral immune cells reveal the immune landscape in human cancer. *Immunity*. 2013;39:782-795. doi:10.1016/j.immuni.2013.10.003. PMID:24138885
 70. Wen L, Ley RE, Volchkov PY, Stranges PB, Avanesyan L, Stonebraker AC, Hu C, Wong FS, Szot GL, Bluestone JA, et al. Innate immunity and intestinal microbiota in the development of Type 1 diabetes. *Nature*. 2008;455:1109-1113. doi:10.1038/nature07336. PMID:18806780
 71. Lee SH, Hu LL, Gonzalez-Navajas J, Seo GS, Shen C, Brick J, Herdman S, Varki N, Corr M, Lee J, et al. ERK activation drives intestinal tumorigenesis in Apc(min/+) mice. *Nature Medicine*. 2010;16:665-670. doi:10.1038/nm.2143. PMID:20473309
 72. Salcedo R, Worschech A, Cardone M, Jones Y, Gyulai Z, Dai RM, Wang E, Ma W, Haines D, O'hUigin C, et al. MyD88-mediated signaling prevents development of adenocarcinomas of the colon: role of interleukin 18. *The Journal of Experimental Medicine*. 2010;207:1625-1636. doi:10.1084/jem.20100199. PMID:20624890
 73. Kinross JM, Darzi AW, Nicholson JK. Gut microbiome-host interactions in health and disease. *Genome Med*. 2011;3:14. doi:10.1186/gm228. PMID:21392406
 74. Chung H, Kasper DL. Microbiota-stimulated immune mechanisms to maintain gut homeostasis. *Curr Opin Immunol*. 2010;22:455-460. doi:10.1016/j.coi.2010.06.008. PMID:20656465
 75. Lee YK, Mazmanian SK. Has the microbiota played a critical role in the evolution of the adaptive immune system? *Science*. 2010;330:1768-1773. doi:10.1126/science.1195568. PMID:21205662
 76. Kuczynski J, Costello EK, Nemergut DR, Zaneveld J, Lauber CL, Knights D, Koren O, Fierer N, Kelley ST, Ley RE, et al. Direct sequencing of the human microbiome readily reveals community differences. *Genome Biol*. 2010;11:210. doi:10.1186/gb-2010-11-5-210. PMID:20441597
 77. Arthur JC, Jobin C. The struggle within: microbial influences on colorectal cancer. *Inflamm Bowel Dis*. 2011;17:396-409. doi:10.1002/ibd.21354. PMID:20848537
 78. Candela M, Guidotti M, Fabbri A, Brigidi P, Franceschi C, Fiorentini C. Human intestinal microbiota: cross-talk with the host and its potential role in colorectal cancer. *Crit Rev Microbiol*. 2011;37:1-14. doi:10.3109/1040841X.2010.501760. PMID:20874522
 79. Ley RE, Hamady M, Lozupone C, Turnbaugh PJ, Ramey RR, Bircher JS, Schlegel ML, Tucker TA, Schrenzel MD, Knight R, et al. Evolution of mammals and their gut microbes. *Science*. 2008;320:1647-1651. doi:10.1126/science.1155725. PMID:18497261
 80. Belizario JE, Napolitano M. Human microbiomes and their roles in dysbiosis, common diseases, and novel therapeutic approaches. *Front Microbiol*. 2015;6:1050. doi:10.3389/fmicb.2015.01050. PMID:26500616
 81. Derrien M, Vaughan EE, Plugge CM, de Vos WM. *Akkermansia muciniphila* gen. nov., sp. nov., a human intestinal mucin-degrading bacterium. *International Journal of Systematic and Evolutionary Microbiology*. 2004;54:1469-1476. doi:10.1099/ijs.0.02873-0. PMID:15388697
 82. Collado MC, Derrien M, Isolauri E, de Vos WM, Salminen S. Intestinal integrity and *Akkermansia muciniphila*, a mucin-degrading member of the intestinal microbiota present in infants, adults, and the elderly. *Applied and Environmental Microbiology*. 2007;73:7767-7770. doi:10.1128/AEM.01477-07. PMID:17933936
 83. Derrien M, Collado MC, Ben-Amor K, Salminen S, de Vos WM. The Mucin degrader *Akkermansia muciniphila* is an abundant resident of the human intestinal tract. *Applied and Environmental Microbiology*. 2008;74:1646-1648. doi:10.1128/AEM.01226-07. PMID:18083887
 84. Weir TL, Manter DK, Sheflin AM, Barnett BA, Heuberger AL, Ryan EP. Stool Microbiome and Metabolome Differences between

- Colorectal Cancer Patients and Healthy Adults. *PloS One*. 2013;8: e70803. doi:10.1371/journal.pone.0070803. PMID:23940645
85. Zella GC, Hait EJ, Glavan T, Gevers D, Ward DV, Kitts CL, Korzenik JR. Distinct microbiome in pouchitis compared to healthy pouches in ulcerative colitis and familial adenomatous polyposis. *Inflammatory Bowel Diseases*. 2011;17:1092-1100. doi:10.1002/ibd.21460. PMID:20845425
86. Yang K, Popova NV, Yang WC, Lozonschi I, Tadesse S, Kent S, Bancroft L, Matisse I, Cormier RT, Scherer SJ, et al. Interaction of Muc2 and Apc on Wnt signaling and in intestinal tumorigenesis: potential role of chronic inflammation. *Cancer Res*. 2008. 68:7313-7322. doi:10.1158/0008-5472.CAN-08-0598. PMID:18794118
87. Medzhitov R. Inflammation 2010: new adventures of an old flame. *Cell*. 2010;140:771-776. doi:10.1016/j.cell.2010.03.006. PMID:20303867